A–π–D–π–A Electron-Donating Small Molecules for Solution-Processed Organic Solar Cells: A Review

Zhen Wang, Lingyun Zhu,* Zhigang Shuai, and Zhixiang Wei*

Organic solar cells based on semiconducting polymers and small molecules have attracted considerable attention in the last two decades. Moreover, the power conversion efficiencies for solution-processed solar cells containing A–π–D–π–A-type small molecules and fullerenes have reached 11%. However, the method for designing high-performance, photovoltaic small molecules still remains unclear. In this review, recent studies on A–π–D–π–A electron-donating small molecules for organic solar cells are introduced. Moreover, the relationships between molecular properties and device performances are summarized, from which inspiration for the future design of high performance organic solar cells may be obtained.

1. Introduction

Solar cells are one of the most promising and effective technologies for converting light to energy. Organic solar cells (OSCs) based on semiconducting polymers and small molecules (SMs) have attracted considerable attention in the past two decades because of their remarkable advantages, such as light weight, simple fabrication, low cost, and flexibility.[1] Power conversion efficiencies (PCEs) of solution-processed single junction bulk-heterojunction (BHJ) OSCs have exceeded over 13% and 11% for polymers and small molecules, respectively.[2] In the last two decades, π-conjugated polymers as electron-rich materials for BHJ solar cells have attracted attention from numerous researchers and have led the performance of OSCs. Polymers usually have high molecular weights that lead to a slow aggregation speed during solvent volatilization.

Therefore, the morphology of active layers can be easily controlled using different solvents and solvent additives. However, compared with polymers, small molecules tend to exhibit higher crystallinity and aggregate quickly to form larger domains, as well as smaller area of donor–acceptor (D–A) interfaces, which are unfavorable for exciton dissociation and charge transfer. Low boiling point solvents, such as chloroform, are used to control aggregation speed. Moreover, films with better molecular π–π stacking usually show high charge carrier mobility. In addition, high crystallinity is beneficial to low energetic disorders and narrow density of state (DOS) distributions. Thus, high open circuit voltage (V_{OC}) is obtained by small molecule solar cells because it is determined by the difference between the lowest unoccupied molecular orbital (LUMO) of the acceptor and the highest occupied molecular orbital (HOMO) of the donor and affected by various factors.[3] Furthermore, using small molecules to fabricate solar cells can accurately avoid the effects induced by the distributions of molecular weights. To obtain high PCEs, considerable efforts have been made to design and synthesize various electron-donating small molecules.

In 1997, Roncali proposed the design principle to tune the molecular bandgap, which combined D and A with different π-conjugated bridges and adjusting HOMO and LUMO levels by changing D and A with different electron-donating strengths and electron-withdrawing strengths, respectively.[4] Recently, inspired by D–A-type π-conjugated copolymers, researchers designed different kinds of small molecules composed of various D and A moieties, and π-conjugated bridges (sometimes called π-conjugated spacers) to adjust the planarity and electronic structures.[5] Electron-donating small molecules can be classified into several types: A–D–A,[6] D–A–D,[7] A1–D–A2–D–A1,[8] D1–A–D2–A–D1,[9] A1–A2–D–A2–A1,[10] D–π–A–π–D,[11] and A–π–D–π–A.[12] Especially, OSCs based on A–π–D–π–A-type small molecules as donors and fullerene derivatives as acceptors exhibit the best performance with PCE of over 11%.[2b] **Figure 1** shows the schematic of A–π–D–π–A structure. Actually, the π-conjugated bridges usually play the function of adjusting the electronic structures in SMs. If the π-conjugated bridge units are regarded as parts of the donor moiety, then A–π–D–π–A-type SMs are similar to A–D–A SMs. Moreover, PCEs of OSCs mainly depend on the electronic structure of molecules and morphology of active layers. What is the reason behind the better performance of A–π–D–π–A-type small molecules than those of other types of small molecules? Thus,

Z. Wang, Dr. L. Zhu, Prof. Z. Wei
CAS Key Laboratory of Nanosystem and Hierarchical Fabrication
CAS Center for Excellence in Nanoscience
National Center for Nanoscience and Technology
Beijing 100190, P. R. China
E-mail: zhuly@nanoctr.cn; weizx@nanoctr.cn

Z. Wang, Prof. Z. Shuai
MOE Key Laboratory of Organic Optoelectronics
and Molecular Engineering
Department of Chemistry
Tsinghua University
Beijing 100084, P. R. China

Z. Wang, Prof. Z. Wei
University of Chinese Academy of Sciences
Beijing 100049, P. R. China

The ORCID identification number(s) for the author(s) of this article can be found under https://doi.org/10.1002/marc.201700470.
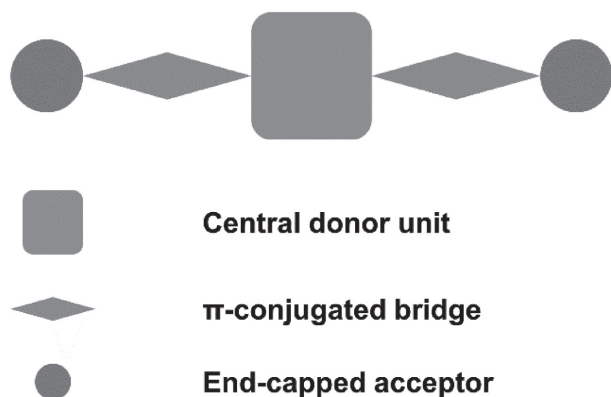
1700470 (1 of 18)

**ADVANCED
SCIENCE NEWS**
www.advancedsciencenews.com

**Macromolecular
Rapid Communications**
www.mrc-journal.de

Central donor unit

π-conjugated bridge

End-capped acceptor

Figure 1. Schematic of A–π–D–π–A structure.

Zhen Wang received his B.S. degree in Applied Physics from the University of Science and Technology, Beijing, in 2014. He is now a joint Ph.D. student at the National Center for Nanoscience and Technology (NCNST) and Department of Chemistry, Tsinghua University, under the supervision of Prof. Zhixiang Wei and Prof. Zhigang Shuai. His research interests are focused on device research and theoretical simulations of organic solar cells.

Lingyun Zhu received her Ph.D. degree from the Institute of Chemistry, Chinese Academy of Sciences, in 2008. From 2008 to 2012, she conducted postdoctoral research at Georgia Institute of Technology, USA, with Prof. Jean-Luc Brédas. She has been an Associate Professor at NCNST since 2013. Her research interests are focused on theoretical simulations of organic solar cells and charge transport properties in organic molecular crystals.

Zhixiang Wei has been a professor at NCNST since 2006. He graduated with a B.S. degree in 1997 and an M.S. degree in 2000 from Xi'an Jiaotong University. He obtained his Ph.D. degree in 2003 from the Institute of Chemistry, Chinese Academy of Sciences. From 2003 to 2005, he undertook postdoctoral research at the Max Planck Institute of Colloids and Interfaces and the University of Toronto. His research focuses on self-assembled organic functional nanomaterials and related flexible devices.

investigating the structure-to-property relationship between molecular structure properties and device performance is necessary.

In this review, we present a brief summary of the recent advances on OSCs based on A–π–D–π–A-type small molecules. Furthermore, statistic summaries between molecular properties and device performances are proposed. Moreover, insights on designing and optimizing small molecules for OSCs for obtaining high efficiencies are provided.

2. Structures of A–π–D–π–A Electron-Donating Small Molecules

2.1. Benzodithiophene-Containing Small Molecules

Benzo[1,2-b:4,5-b']dithiophene (BDT) is the most attractive chemical moiety in solvable A–π–D–π–A small molecules.[5d,12a] In 2011, Liu et al. first introduced BDT as central moiety into a 1D A–π–D–π–A-type small molecule DCAO3T(BDT)3T (**m1**) with a PCE of 5.44%. The results showed a great potential for the BDT and oligothiophene building blocks in creating D–A conjugated small molecules for high performance BHJ solar cells.[13] After that, Zhou et al. synthesized DCAO3TBDT (**m2**) and DR3TBDT (**m3**) molecules, introducing 2-ethylhexoxy substituted BDT. The latter one exhibited a PCE of 6.92% without any post-treatment and a PCE of 7.38% after adding a small amount of polydimethysiloxane to the active layer.[14] Following that, a series of 2D-conjugated small molecules, such as DR3T-BDTT (**m4**), DR3TBDTT-HD (**m5**), and DR3TBDT2T (**m6**) with BDT moiety, were designed and synthesized by the same research group. PCEs of 8.12% and 8.02% were obtained for DR3TBDTT and DR3TBDT2T as donors and 6,6-phenyl-C$_{71}$-butyric acid methyl ester (PC$_{71}$BM) as the acceptor. The high PCE mainly benefits from the improved short-circuit current density (J_{SC}) without sacrificing the high V_{oc} and FF through incorporating the advantages of conventional small molecules and polymers.[15] Based on **m3**, Kan et al. changed the 2-ethylhexoxy moiety into dialkylthiol moiety and designed new molecule DR3TSBDT (**m7**). After thermal annealing and solvent vapor annealing, devices based on this molecule showed a remarkably high PCE of 9.95%.[16] Moreover, based on thieno[3,2-b]thiophene-substituted benzo[1,2-b:4,5-b']dithiophene, they designed

a small molecule DRBDT-TT (**m8**) with alkyl side chains and a DRBDT-STT (**m9**) with alkylthio side chains. Both molecules exhibited good thermal stability, suitable energy levels, and ordered molecular packing. When the alkyl chain was replaced by the alkylthio side chain, the dihedral angle between the thieno[3,2-b]thiophene and BDT moiety was increased; thus, the intermolecular interaction was slightly reduced, which led to a blue-shifted absorption in the solid film.[17] Cui et al. reported a new 2D-conjugated small donor molecule BDTT-S-TR (**m10**) with alkylthio-thienyl-substituted BDT as the central unit, and

ADVANCED
SCIENCE NEWS
www.advancedsciencenews.com

Macromolecular
Rapid Communications
www.mrc-journal.de

the BHJ OSCs based on BDTT-S-TR/PC$_{71}$BM demonstrated a high PCE of 9.20% without any extra treatment.[18] Later, Min et al. designed and synthesized three small molecules based on thienyl-substituted benzo[1,2-b:4,5-b']dithiophene (BDTT) units with different linking atoms to their alkyl side chains, including BDTT-TR (m4), BDTT-O-TR (m11), and BDTT-S-TR (m10). BDTT-based devices with the meta-alkylthio side chain exhibited a higher PCE (9.20%) compared with the meta-alkoxy and meta-alkyl spacer because of a well-defined microstructure combined with high and balanced charge transport properties.[19] Du et al. applied alkoxyphenyl-substituted benzo BDT unit (namely BDTP) as the central core to a new 2D-conjugated small molecule DCA3TBDTP (m12), which performed a PCE of 4.51% with a high V_{OC} value of 0.90 V after thermal annealing at 70 °C.[20]

Multitudinous efforts have been made to optimize the SMs through changing the end-capped units. As mentioned above, Zhou et al. designed m2 by replacing the end-capped unit of octyl cyanoacetate by 3-ethylrhodanine. The absorption ability was improved significantly, and thus, the devices based on the corresponding compound m3 exhibited considerably higher J_{SC}.[14] Liu et al. obtained a PCE of 8.1% with small molecule SMPV1 (m13) containing 3-octylrodanine as the electron-withdrawing end-group.[21] Fan et al. introduced 2-(1,1-dicyanomethylene)rhodanine (DCRD) as an electron-withdrawing end-group into BDT- and BDTT-based SMs, which were denoted as D(T$_3$-DCRD)-BDT (m14) and D(T$_3$-DCRD)-BDTT (m15), respectively. Both compounds exhibited broad absorption in the range of 300–750 nm, and PCE values of 1.10% and 1.94% were achieved for OSCs based on the compounds/6,6-phenyl-C$_{61}$-butyric acid methyl ester (PC$_{61}$BM), respectively.[22] Kumar et al. reported a pair of novel molecules DRT3-BDT(1) (m16) comprising rhodanine moiety with ethyl hexyl side chains and DTT3-BDT(2) (m17) containing thiazolidione moiety with ethylhexyl side chains. Device based on m16 yielded a PCE value of 6.76% because of its improved nanoscale phase separation, smooth surface, and high carrier mobility, whereas those based on m17 exhibited a low PCE value of 5.25%.[23]

Our group investigated the effects of different electron-withdrawing end caps on the device properties of A–π–D–π–A SMs. In 2014, we designed and synthesized two new molecules, DOO3OTTBDT (m18) and DOP3HTTBDT (m19), by shortening alkyl chains of those that attached to π-conjugated bridges and end-capped acceptors. The self-assembly and device performances were improved by shortening the length of the widely used octyl chains. Differential scanning calorimetry and grazing incidence wide angle X-ray scattering (GIWAXS) demonstrated the tight molecular stacking and high crystallinity in the mixture with PC$_{71}$BM; hence, a high PCE value of 5.6% with a V_{OC}, J_{SC}, and fill factor (FF) values of 0.87 V, 9.94 mA cm^{-2}, and 65%, respectively, were obtained.[24] Following that, we designed and synthesized three molecules by introducing subtle structural changed end-capped acceptors with increasing electron-withdrawing abilities, namely BDT3SCNCOO (m20) with octyl 2-cyanoacetate, BDT3SCNCO (m18) with 3-oxoundecanenitrile, and BDT3SCNSOO (m21) with 2-(octylsulfonyl) acetonitrile. The end-capped acceptors significantly affected the absorption in solid films, thermal properties, hole mobility values, and morphologies. The m20

showed a PCE of 6.4% with V_{oc}, J_{sc}, and FF values of 0.89 V, 9.98 mA cm^{-2}, and 72% because of the small steric effect and short π–π stacking distance. The m18 performed a PCE of 6.4% with V_{oc}, J_{sc}, and FF values of 0.92 V, 10.2 mA cm^{-2}, and 68%, while m21 exhibited a PCE of 3.0% with V_{oc}, J_{sc}, and FF values of 0.93 V, a J_{sc} of 6.1 mA cm^{-2}, and a low FF of 52.8% owing to poor crystallinity.[25] Recently, we reported three novel solution-processable small molecules, which contain π-conjugated bridges with gradient-decreased electron density and end acceptors substituted with various fluorine atoms, namely 0F for BTID-0F (m22), 1F for BTID-1F (m23), and 2F for BTID-2F (m24). With incremental introduction of fluorine to end-capped units, the PCE for inverted devices increased from 8.30% for m22 to 10.4% for m23, and to 11.3% for m24, which to our best knowledge, is the highest PCE reported for A–π–D–π–A SM/PC$_{71}$BM OSCs to date. GIWAXS results illustrated a highly condensed stacking in the π–π direction after fluorination, which was consistent with the red-shifted absorption in films. Interfacial energy disorder was reduced by the good aggregations for PC$_{71}$BM and small molecules, and this was beneficial for lowering the loss of V_{OC}. X-ray photoelectron spectroscopy measurements demonstrated that the fluorine-substituted groups are highly prone to be enriched at the active layer surface. High PCEs can be attributed to a hierarchical morphology with high domain purity, enhanced surface enrichment, and high directional vertical phase distribution induced by fluorine substitute.[2b]

In addition to the central building block and end cap, π-conjugated bridge plays an important role in A–π–D–π–A SMs. In 2013, Shen et al. designed molecules D1 (m25), D2 (m26), DO1 (m27), and DO2 (m28) with BDTT and alkoxy side chains on BDT as donor units, respectively, and indenedione (ID) as electron-withdrawing end groups. The influence of π-bridges was further studied, and the results indicated that bithiophene π-bridges demonstrate stronger absorbance and higher hole mobility values than the compounds with thiophene π-bridges.[26] Targeting the oligothiophene π-bridges, Tang et al. reported a series of BDTT and electron-deficient quinoidal methyldioxocyano-pyridine-based SMs with oligothiophene (0T–5T, m29–m36) π-bridges. As they declared, the quinoidal structure enhanced the photoinduced intramolecular charge transfer, leading to the absorbance enhancement of the low-energy absorption band. With the increased size of the oligothiophene from 0 to 5 thienyl units and the change of the direction of the alkyl chains on the bridged thiophene from "outward" to "inward," the crystalline nature, fibril length, and phase size of the blend films, as well as the cell performance, were all finely tuned. With the "inward" alkyl chains, the terthiophene-bridged molecule was amorphous, whereas the pentathiophene-bridged one was relatively crystalline.[27]

Device engineering contributes to high performances of BDT containing small molecule OSCs through optimizing the morphology of the active layer. Ni et al. designed and synthesized small molecule DR3TDOBDT (m37) containing 4,8-dioctyl benzo[1,2-b:4,5-b0]dithiophene as the central block and 3-(2-ethylhexyl)-rhodanine as the end-capped groups. Without any post-treatment, devices showed a low PCE of 4.34%. After thermal annealing, PCE values were enhanced to 6.53%. When thermal annealing and solvent vapor treatment were used,

**ADVANCED
SCIENCE NEWS**
www.advancedsciencenews.com

**Macromolecular
Rapid Communications**
www.mrc-journal.de

a high PCE of 8.26% was achieved.[28] Li et al. systematically studied the performances of **m4**/PC$_{71}$BM based OSCs under different solvent vapor treatments. Carbon disulfide (CS$_2$), chloroform (CHCl$_3$), tetrahydrofuran, and methylene chloride (CH$_2$Cl$_2$) with different solubilities for D/A materials and different boiling points were used. Solvents with high vapor pressures, as they claimed, could crystallize donor molecules, leading to increased length scale of phase separation and improved domain purity, which are beneficial for enhancing the device performance.[29]

Figure 2 and Figure 3 shows the chemical structures of BDT-containing small molecules of **m1**–**m37**. The building block BDT can be introduced into 1D and 2D small molecules as the central building block owing to its unique chemical structures and good physical properties. It usually exhibits good planarity and enhanced electron delocalization, thereby promoting

π–π stacking and crystallization in the solid state.[12a] With various side chains, π-bridges and end-capped acceptors, the BDT-containing SMs exhibit a band gap varying from 1.42 to 1.80 eV, a HOMO level of −4.11 to −2.83 eV, and a LUMO level of −5.46 to −5.02 eV (as shown in **Table 1**). We still believe that the BDT-based SMs have great potential in providing better performances, and this needs further exploration.

2.2. Oligothiophene-Containing Small Molecules

Thiophene, the most common and widely used moiety in organic photovoltaic (OPV) donor materials, usually plays an important role in π-conjugated bridges. However, impressive performances were obtained with thiophene functions as the donor moiety in A–π–D–π–A SMs. Actually, under these
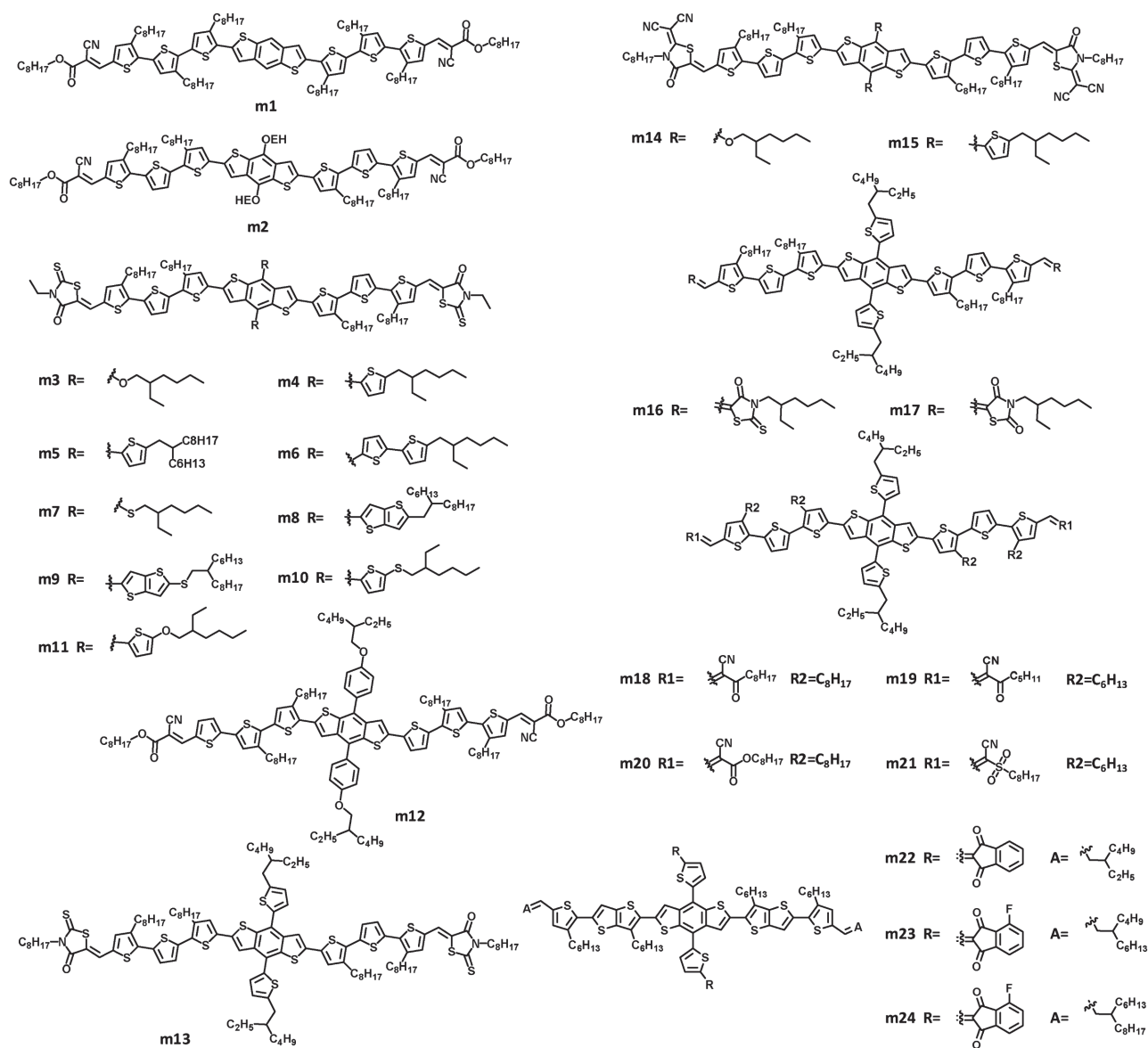

Figure 2. Chemical structures of benzodithiophene-containing small molecules of **m1**–**m24**.
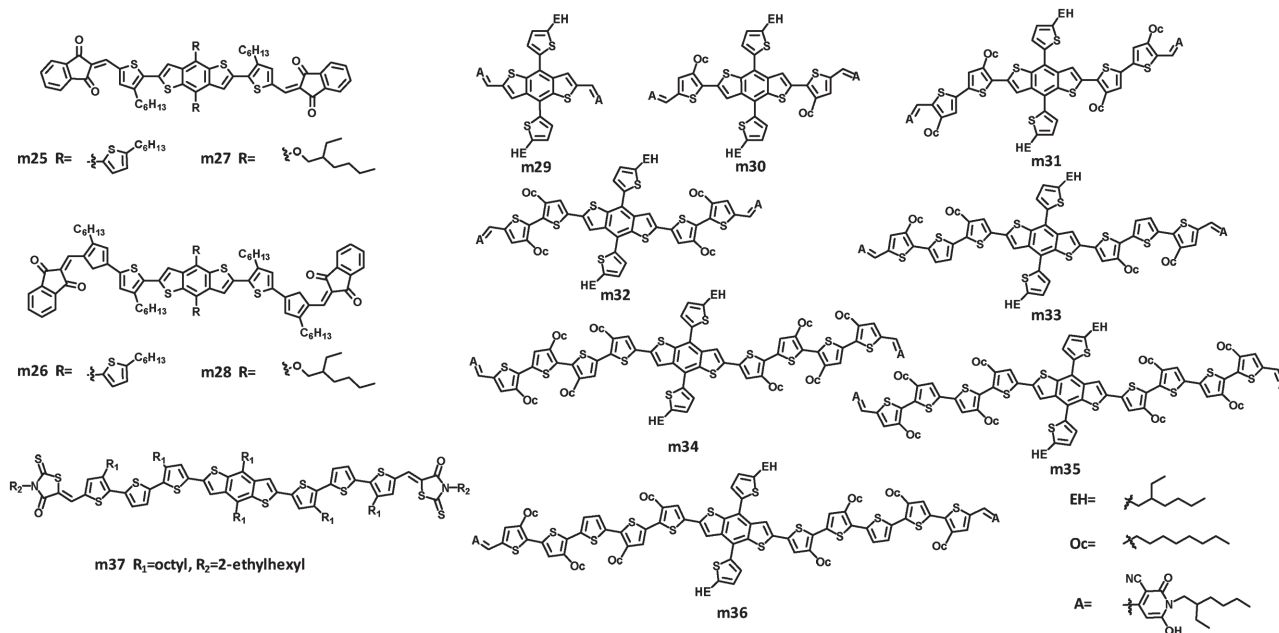
Figure 3. Chemical structures of benzodithiophene-containing small molecules of **m25–m37**.

circumstances, no obvious borderlines were observed between donor moieties and π-bridges. Earlier in 2006, Schulze et al. introduced an oligothiophene-containing SM called DCV5T to fabricate vacuum-deposited bilayer OSCs and achieved a PCE of 3.4%.[30] In 2011, for solution-processed OSCs, Liu et al. designed and synthesized three oligothiophene-based small molecules with different electron-withdrawing alkyl cyanoacetate groups, namely DCAE7T (**m38**), DCAO7T (**m39**), and DCAEH7T (**m40**), that exhibited PCEs of 4.46–5.08%.[31] Based on this work, a series of research explorations were conducted by replacing the end-capped groups, because end groups can serve as π-stacking regulators, which provide easier routes for adjusting the aggregation. Li et al. introduced 3-ethylrhodanine into the targeted OPV molecule named DERHD7T (**m41**), which showed strong solar light absorption, a remarkable J_{SC} of 13.98 mA cm^{-2}, and a high PCE of 6.10% blended with PC$_{61}$BM.[32] He et al. tried to use 1,3-indanedione (IN) (**m42**), [1,2']biindenylidene-3,10,30-trione (DIN) (**m43**), and 2-(3-oxo-2,3-dihydroinden-1-ylidene)malononitrile (INCN) (**m44**) as the end acceptor moieties. Among them, DIN7T/ PC$_{61}$BM OSCs showed a PCE of 4.93%, whereas DDIN7T/ PC$_{61}$BM exhibited a low PCE because of poor packing in the solid state.[33] Zhang et al. reported a small molecule DRCN7T (**m45**) with 2-(1,1-dicyanomethylene)rhodanine as the terminal unit. Devices based on DRCN7T/PC$_{71}$BM exhibited impressive optimized PCE of 9.30% with a nearly 100% internal quantum efficiency. After thermal annealing, **m45** showed a broader and generally stronger absorption than **m41**. Enhanced crystallinity and effective π–π stacking between the molecular backbones were observed.[34] Moreover, time-of-flight and organic field-effect transistor were applied to study the influences of molecular structure, trap states, and molecular orientation on charge transport of small-molecule **m41** and **m45**.[35] Long et al. designed and synthesized three quinquethiophene derivatives with different end groups of octyl 2-cyanoacetate

(DCAO5T, **m46**), 3-ethylrhodanine (DERHD5T, **m47**), and 2H-indene-1,3dione (DIN5T, **m48**). Among them, DERHD5T/ PC$_{61}$BM-based devices showed a V_{OC} as high as 1.08 V and a PCE of 4.63%, owing to a deep HOMO and a weak interaction between DERHD5T and PC$_{61}$BM.[36] Kan et al. systematically investigated the effect of oligothiophene length on the properties of 2-(1,1-dicyanomethylene)rhodanine-based SMs, namely, DRCN4T-DRCN9T (**m49–m51**, **m45**, **m52**, and **m53**). The devices based on DRCN5T, DRCN7T, and DRCN9T with axisymmetric chemical structures exhibited considerably higher J_{SC} densities than those based on DRCN6T and DRCN8T with centrosymmetric chemical structures, which is attributed to their well-developed fibrillar network with a feature size of less than 20 nm. The devices based on DRCN5T/PC$_{71}$BM showed a notably certified PCE of 10.10% under AM 1.5 G irradiation (100 mW cm^{-2}).[37] Further studies revealed that the amorphous morphology in the lack of percolated pathways leads to the formation of strongly bound charge transfer states, which accounts for about one third of the photoexcited species.[38]

Efforts have been made to replace the central block of oligothiophene containing SMs. Zhang et al. introduced thieno[3,2-b]thiophene (TT) as the central building block to substitute the bithiophene group in DRCN8T (**m52**). The new molecule DRCN8TT (**m54**) exhibited an optimized PCE of 8.11%, which was attributed to the improved morphology of small and high crystalline domains that were nearly commensurate with the excitation diffusion length.[39] Based on DRCN7T (**m45**), Zuo et al. synthesized the small molecule DRCN7T-Se (**m55**) with selenophene as central moiety. Owing to the large diameter of fibril-like domains, a low PCE of 8.30% was achieved.[40] Liu et al. designed and synthesized oligothiophene-based small molecules, STDR (**m56**) and STDR-TbT (**m57**), which contain the quinoid structure 2-ethylhexyl 3-fluorothieno[3,4-b]thiophene-2-carboxylate as the central block. Devices based on STDR/PC$_{71}$BM showed a PCE of 2.31% and those based on

Table 1. Photophysical and device performance parameters of **m1–m37**.

SM	Acceptor	E_g^{opt} [eV]	HOMO [eV]	LUMO [eV]	μ_h [cm^2 V^{-1} s^{-1}]	V_{OC} [V]	J_{SC} [mA cm^{-2}]	FF [%]	PCE [%]	References
m1	PC$_{61}$BM	1.74	−5.11	−3.54	4.50×10^{-4}	0.92	8.25	64.2	4.87	[13]
m2	PC$_{61}$BM	1.84	−5.04	−3.24	1.38×10^{-4}	0.95	8.00	60.0	4.56	[14]
m2	PC$_{71}$BM	1.84	−5.04	−3.24	1.38×10^{-4}	0.93	3.74	60.1	2.09	[14]
m3	PC$_{61}$BM	1.74	−5.02	−3.27	1.76×10^{-4}	0.91	10.78	65.0	6.38	[14]
m3	PC$_{71}$BM	1.74	−5.02	−3.27	1.76×10^{-4}	0.93	12.21	65.0	7.38	[14]
m4	PC$_{71}$BM	1.72	−5.02	−3.27	2.88×10^{-4}	0.93	13.17	66.3	8.12	[15]
m5	PC$_{71}$BM	1.76	−5.06	−3.29	1.52×10^{-4}	0.96	11.92	59.4	6.79	[15]
m6	PC$_{71}$BM	1.76	−5.07	−3.29	3.29×10^{-4}	0.92	12.09	72.1	8.02	[15]
m7	PC$_{71}$BM	1.74	−5.07	−3.30	6.13×10^{-4}	0.91	14.45	73.0	9.60	[16]
m8	PC$_{71}$BM	1.78	−5.13	−3.33	5.41×10^{-4}	0.91	12.93	71.0	8.70	[17]
m9	PC$_{71}$BM	1.80	−5.15	−3.34	4.74×10^{-4}	0.90	12.20	70.0	8.01	[17]
m10	PC$_{71}$BM	1.73	−5.18	−3.25	6.57×10^{-4}	0.97	11.45	70.5	9.20	[18]
m11	PC$_{71}$BM	1.73	−5.14	−3.34	3.70×10^{-4}	0.90	11.03	65.5	6.50	[19]
m12	PC$_{61}$BM	1.82	−5.25	−3.43	2.74×10^{-4}	0.90	7.88	63.7	4.51	[20]
m13	PC$_{71}$BM	1.90	−5.51	−3.64	3.30×10^{-4}	0.94	12.50	69.0	8.10	[21]
m14	PC$_{61}$BM	1.62	−5.39	−2.84	5.07×10^{-5}	0.93	2.44	49.0	1.10	[22]
m15	PC$_{61}$BM	1.61	−5.46	−2.83	6.22×10^{-4}	0.96	3.69	55.0	1.94	[22]
m16	PC$_{71}$BM	1.74	−5.42	−3.54	8.68×10^{-5}	0.90	11.92	63.0	6.76	[23]
m17	PC$_{71}$BM	1.84	−5.38	−3.44	2.94×10^{-5}	0.86	10.52	58.0	5.25	[23]
m18	PC$_{71}$BM	1.76	−5.19	−3.46	1.40×10^{-4}	0.94	8.00	70.0	5.26	[24]
m19	PC$_{71}$BM	1.77	−5.11	−3.37	1.10×10^{-4}	0.87	9.94	65.0	5.65	[24]
m20	PC$_{71}$BM	1.84	−5.08	−3.47	1.20×10^{-4}	0.89	9.98	72.0	6.40	[25]
m21	PC$_{71}$BM	1.85	−5.11	−3.46	1.40×10^{-6}	0.93	6.10	53.0	3.00	[25]
m22	PC$_{71}$BM	1.71	−5.19	−3.49	4.70×10^{-4}	0.93	14.00	64.0	8.30	[2b]
m23	PC$_{71}$BM	1.70	−5.24	−3.47	–	0.94	15.30	72.0	10.40	[2b]
m24	PC$_{71}$BM	1.68	−5.33	−3.46	1.40×10^{-3}	0.95	15.70	76.0	11.30	[2b]
m25	PC$_{71}$BM	1.61	−5.19	−3.56	2.04×10^{-4}	1.03	10.07	54.7	5.67	[26]
m26	PC$_{71}$BM	1.60	−5.16	−3.54	1.71×10^{-4}	0.92	11.05	66.4	6.75	[26]
m27	PC$_{71}$BM	1.59	−5.18	−3.56	2.82×10^{-4}	0.91	9.47	48.2	4.15	[26]
m28	PC$_{71}$BM	1.60	−5.16	−3.52	2.63×10^{-4}	0.92	8.58	64.8	5.11	[26]
m29	PC$_{71}$BM	1.42	−5.13	−4.11	9.06×10^{-6}	0.64	0.10	31.5	0.02	[27]
m30	PC$_{71}$BM	1.46	−5.11	−3.84	6.07×10^{-5}	0.82	3.41	33.2	0.95	[27]
m31	PC$_{71}$BM	1.46	−5.10	−3.80	2.37×10^{-5}	0.79	6.48	35.1	1.85	[27]
m32	PC$_{71}$BM	1.48	−5.09	−3.75	2.37×10^{-5}	0.81	6.16	30.4	1.56	[27]
m33	PC$_{71}$BM	1.42	−5.10	−3.75	7.44×10^{-3}	0.79	14.38	55.4	6.29	[27]
m34	PC$_{71}$BM	1.42	−5.06	−3.76	1.27×10^{-5}	0.78	4.91	40.2	1.56	[27]
m35	PC$_{71}$BM	1.56	−5.12	−3.76	1.27×10^{-5}	0.76	2.05	25.2	0.45	[27]
m36	PC$_{71}$BM	1.42	−5.10	−3.74	4.00×10^{-3}	0.81	9.62	68.7	5.35	[27]
m37	PC$_{71}$BM	1.81	−5.08	−3.27	4.08×10^{-4}	0.94	12.56	70.0	8.26	[28]

STDR-TbT/PC$_{71}$BM yield a high PCE of 5.05% for its high J_{sc} resulting from the significant bathochromic shift with a low optical bandgap in the thin film.[41]

Inspired from the famous polymer P3HT, oligothiophene-based small molecules usually exhibit deep LUMO levels and hence, narrow band gaps (as shown in **Table 2**) and reach PCE values over 10%.[37] Therefore, even with simple molecular structures, impressive performances can be obtained. Chemical structures of thiophene-containing small molecules of **m38–m57** are shown in **Figure 4**.

ADVANCED
SCIENCE NEWS
www.advancedsciencenews.com

Macromolecular
Rapid Communications
www.mrc-journal.de

Table 2. Photophysical and device performance parameters of **m38**–**m57**.

SM	Acceptor	E_g^{opt} [eV]	HOMO [eV]	LUMO [eV]	μ_h [cm^2 V^{-1} s^{-1}]	V_{OC} [V]	J_{SC} [mA cm^{-2}]	FF [%]	PCE [%]	References
m38	PC$_{61}$BM	1.73	−5.09	−3.33	4.51×10^{-4}	0.88	9.94	51.0	4.46	[31]
m39	PC$_{61}$BM	1.74	−5.13	−3.29	3.26×10^{-4}	0.86	10.74	55.0	5.08	[31]
m40	PC$_{61}$BM	1.75	−5.10	−3.26	1.94×10^{-4}	0.93	9.91	49.1	4.52	[31]
m41	PC$_{61}$BM	1.72	−5.00	−3.28	1.50×10^{-4}	0.92	13.98	47.4	6.10	[32]
m42	PC$_{61}$BM	1.49	−4.97	−3.44	1.73×10^{-4}	0.80	8.56	72.0	4.93	[33]
m43	PC$_{61}$BM	1.20	−4.90	−3.86	3.00×10^{-5}	0.76	3.14	28.0	0.66	[33]
m44	PC$_{61}$BM	1.33	−5.02	−3.72	–	–	–	–	–	[33]
m45	PC$_{71}$BM	1.62	−4.95	−3.36	5.91×10^{-4}	0.91	14.87	68.7	9.30	[34]
m46	PC$_{61}$BM	1.80	−5.25	−3.23	3.94×10^{-4}	0.88	7.02	53.0	3.27	[38]
m47	PC$_{61}$BM	1.65	−5.09	−3.20	3.86×10^{-4}	1.02	9.26	49.0	4.63	[38]
m48	PC$_{61}$BM	1.56	−5.11	−3.36	5.51×10^{-4}	0.78	8.13	63.0	4.00	[38]
m49	PC$_{71}$BM	1.77	−5.34	−3.46	–	–	–	–	–	[37]
m50	PC$_{71}$BM	1.60	−5.22	−3.41	6.54×10^{-4}	0.92	15.66	68.0	10.08	[37]
m51	PC$_{71}$BM	1.60	−5.16	−3.56	–	0.92	11.45	58.0	6.33	[37]
m52	PC$_{71}$BM	1.61	−5.02	−3.45	5.77×10^{-4}	0.86	10.80	68.0	6.50	[37]
m53	PC$_{71}$BM	1.59	−4.97	−3.44	5.11×10^{-4}	0.81	13.77	68.0	7.86	[37]
m54	PC$_{71}$BM	1.62	−5.08	−3.46	6.40×10^{-4}	0.88	14.07	65.5	8.11	[39]
m55	PC$_{71}$BM	1.62	−5.05	−3.43	2.30×10^{-4}	0.91	13.06	69.6	8.30	[40]
m56	PC$_{71}$BM	1.70	−5.09	−3.23	1.38×10^{-4}	0.87	6.09	42.9	2.31	[41]
m57	PC$_{71}$BM	1.60	−5.01	−3.29	2.42×10^{-5}	0.76	10.90	61.4	5.05	[41]

2.3. Porphyrin-Containing Small Molecules

Porphyrins and related materials have attracted considerable attention in OSCs because of their strong absorption in both the blue (Soret or B-band) and red (Q-bands) parts of the visible spectrum, as well as high thermal stability.[42] Recently, researchers have tried using porphyrins as the donor moiety in A–π–D–π–A SMs. In 2015, Arrechea et al. designed and synthesized two compounds (**m58**–**m59**) with Zn-porphyrin functioning as the donor and linked by ethynylenes to one or two units of thienylenevinylene and capped by dicyanovinylene groups as acceptor units. Blended with PC$_{61}$BM, the compounds performed PCEs of 1.48% and 2.82%, respectively, and PCEs of 1.34% and 3.16% were obtained with PC$_{71}$BM, respectively.[43] Kumar et al. reported a porphyrin molecule with ethyl rhodanine end-capped groups and octyl thiophene-ethynylene as π-bridges, namely VC117 (**m60**), which exhibited an optimized PCE of 5.50% with V_{OC}, J_{SC}, and FF values of 0.76 V, 11.67 mA cm^{-2}, and 62%.[44] Gao et al. reported two SMs Por-Rod (**m61**) and Por-CNRod (**m62**) using porphyrin core as the donor and 3-ethylrhodanine and 2-(1,1-dicyanomethylene)rhodanine as acceptor units. Por-Rod showed a stronger and red-shifted absorption compared with Por-CNRod and other nonfunctionalized porphyrins; thus, an optimized PCE of 4.97% with a high J_{SC} value of 12.39 mA cm^{-2} was obtained.[45] Wang et al. developed three comparable porphyrin-based small molecules (**m63**–**m65**) by introducing 3-ethylrhodanine as the acceptor moiety and 5,15-bis(phenylethynyl) as the bridge. As declared, molecule with 10,20-bis(2-hexylnonyl) aliphatic peripheral substituent on porphyrin core exhibited strong intermolecular π–π stacking and high charge carrier mobility; hence, a higher PCE of 7.70% was obtained compared with those with 10,20-bis[3,5di(dodecyloxy)phenyl] and 10,20-bis(4-dodecyloxylphenyl substituents.[46] Xiao et al. designed and synthesized two SMs, PTTR (**m66**) and PTTCNR (**m67**), using porphyrin-core with the vertical aliphatic 2-octylundecyl peripheral substitutions as donor and 3-ethylrhodanine and 2-(1,1-dicyanomethylene) rhodanine as acceptor units by linking through terthiophenes, respectively. Both performed excellently (with PCE values of 7.66% and 8.21%) as a result of increased solar flux coverage in the visible and near-infrared region.[47]

Coming from the chlorophyll, high hopes have been placed on porphyrins. Porphyrin-based polymer solar cells have yielded a PCE of 8.6%.[48] Moreover, porphyrin-containing A–π–D–π–A small-molecule solar cells exceeded a PCE of 8.21% (as shown in **Table 3**).[47] Chemical structures of porphyrin-containing small molecules of **m58**–**m67** are shown in **Figure 5**. However, porphyrin-containing molecules need further investigation.

2.4. Dithienosilole-Containing Small Molecules

Dithieno[3,2-b:2′,3′-d]silole (DTS) as donor moiety was first used in D1–A–D2–A–D1-type small molecule DTS(PTTh$_2$)$_2$ by Sun et al.; it exhibited an impressive PCE of 6.7%.[9a] Realizing its potential in achieving remarkable performances, researchers have introduced DTS into A–π–D–π–A SMs. Zhou et al.

**ADVANCED
SCIENCE NEWS**
www.advancedsciencenews.com

**Macromolecular
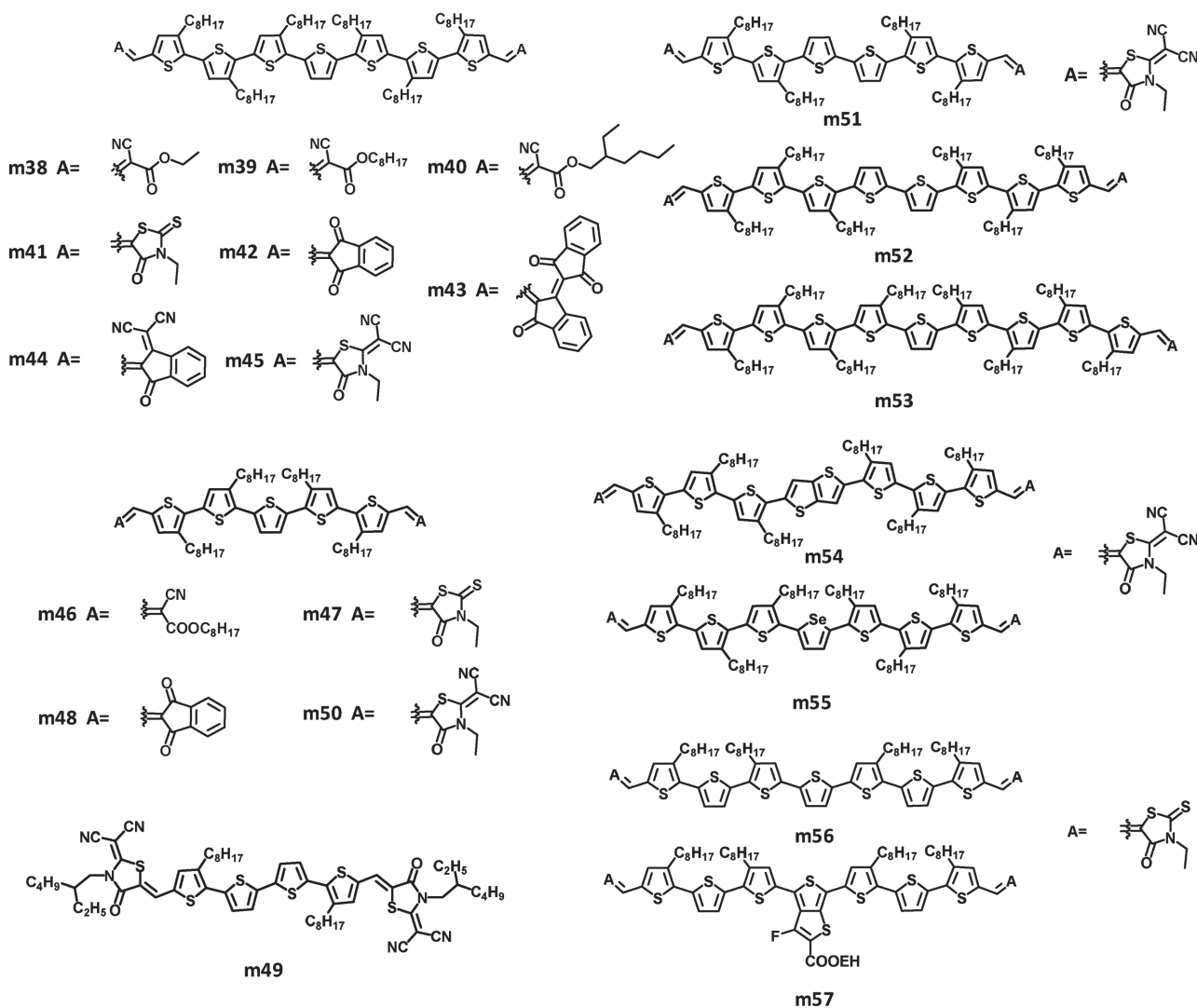Rapid Communications**
www.mrc-journal.de

Figure 4. Chemical structures of oligothiophene-containing small molecules of **m38–m57**.

reported DTS-based small molecule DCAO3TSi (**m68**) with terthiophenes as π-conjugated bridges and octyl cyanoacetate as end-capped acceptors. Devices based on DCAO3TSi/PC$_{61}$BM blend showed a PCE of 5.84%.[49] Fu et al. designed and synthesized SMs DTS(TTPD)$_2$ (**m69**) and DTS(BTTPD)$_2$ (**m70**) with thieno[2,3-c]pyrrole-4,6-dione (TPD) units as end caps. Solar cells using DTS(TTPD)$_2$ as donor and PC$_{61}$BM as acceptor demonstrated a high V_{OC} value of 0.97 V and a PCE of 1.20% after annealing.[50] Kim et al. reported a series of DTS-based SMs (**m71–m76**) with different terminal groups of ester and amide groups combined with three different alkyl side chains. The effects of intermolecular interactions on their structural, optical, and electrical properties were investigated. The blend films of C8-Ester/PC$_{61}$BM and C10-Ester/PC$_{61}$BM produced an optimized PCE exceeding 4.3% for their bi-continuous BHJ morphologies with well-defined interfaces and domain size.[51] Ye et al. developed three SMs (**m77–m79**) consisting of DTS as the central unit and bithiophene bridges with different alkyl group substituents and octyl cyanoacetate or dicyano unit as different end-capped acceptors. BHJ devices based on

SMs/PC$_{61}$BM demonstrated PCEs of 3.27%, 2.88%, and 3.81%.[52] Min et al. synthesized a series of SMs (**m80–m85**) bearing DTS unit linked through bithiophene π-bridges with electron-withdrawing alkyldicyanovinyl groups, which revealed the effect of integrated alkyl chain engineering on morphological control. An optimized PCE of 6.4% was achieved for DTS(Oct)$_2$-(2T-DCV-Me)$_2$/PC$_{71}$BM blend.[53]

In addition to the DTS unit, other donor groups similar to DTS have drawn the attention of researchers. In 2014, Wessendorf et al. presented a series of SMs (**m86–m91**) composed of dicyanovinyl (DCV) groups as acceptors and a fused dithieno[3,2-b:2′,3′-d]pyrrole (DTP) as donor, which exhibited PCEs between 4.4% and 6.1% caused by the varying types and positions of the solubilizing alkyl chains.[54] Li et al. introduced dithienopyrrole (DTN) as core units into small molecule DR3TDTN (**m92**) with octyl-rhodanine as the acceptor and terthiophene as the π-bridge, thereby performing a PCE of 3.03%.[55] Luponosov et al. synthesized SMs (**m93–m95**) with alkyldicyanovinyl groups linked through an oligothiophene π-bridge with either dithienosilole or cyclopentadithiophene

ADVANCED
SCIENCE NEWS
www.advancedsciencenews.com

Macromolecular
Rapid Communications
www.mrc-journal.de

Table 3. Photophysical and device performance parameters of **m58**–**m67**.

SM	Acceptor	E_g^{opt} [eV]	HOMO [eV]	LUMO [eV]	μ_h [cm^2 V^{-1} s^{-1}]	V_{OC} [V]	J_{SC} [mA cm^{-2}]	FF [%]	PCE [%]	References
m58	PC$_{61}$BM	1.75	−5.50	−3.76	–	0.86	5.67	28.1	1.48	[43]
m58	PC$_{71}$BM	1.75	−5.50	−3.76	–	0.84	5.56	26.4	1.24	[43]
m59	PC$_{61}$BM	1.69	−5.36	−3.67	–	0.82	9.44	35.0	2.70	[43]
m59	PC$_{71}$BM	1.69	−5.36	−3.67	–	0.82	10.83	35.7	3.16	[43]
m60	PC$_{71}$BM	1.77	−5.13	−3.36	8.45×10^{-5}	0.76	11.67	62.0	5.50	[44]
m61	PC$_{71}$BM	1.47	−5.24	−3.77	8.50×10^{-5}	0.94	12.39	42.7	4.97	[45]
m62	PC$_{71}$BM	1.45	−5.32	−3.87	7.50×10^{-6}	0.94	2.43	26.4	0.60	[45]
m63	PC$_{61}$BM	1.60	−5.19	−3.59	–	0.76	6.44	29.0	1.42	[46]
m63	PC$_{71}$BM	1.60	−5.19	−3.59	1.57×10^{-5}	0.90	7.20	48.1	3.21	[46]
m64	PC$_{61}$BM	1.55	−5.15	−3.60	–	0.80	10.09	56.3	4.55	[46]
m64	PC$_{71}$BM	1.55	−5.15	−3.60	8.48×10^{-5}	0.90	10.14	55.6	5.07	[46]
m65	PC$_{61}$BM	1.60	−5.12	−3.52	–	0.89	12.14	48.1	5.20	[46]
m65	PC$_{71}$BM	1.60	−5.12	−3.52	2.18×10^{-5}	0.91	13.32	63.6	7.70	[46]
m66	PC$_{71}$BM	1.52	−5.14	−3.56	3.62×10^{-4}	0.80	14.93	64.2	7.66	[47]
m67	PC$_{71}$BM	1.45	−5.17	−3.63	4.14×10^{-4}	0.82	14.30	70.01	8.21	[47]

as donor unit. Changing the bridgehead atom from carbon to silicon in the donor unit led to a significant change in optical, thermal, and structural properties of SMs. Moreover, the HOMO and LUMO energies were increased, and the absorption spectra were blue-shifted because of the elongation of the oligothiophene π-bridge.[56] With 3-ethyl-rhodanine as the end-capped acceptor, Ni et al. designed a pair of SMs DR3TDTC (**m96**) and DR3TDTS (**m97**) with 2,6-(4,4-bis(2-ethylhexyl)-4H-cyclopenta[2,1-b;3,4-b']-dithiophene (DTC) and DTS as donor units, respectively. Device based on DR3TDTS/PC$_{71}$BM
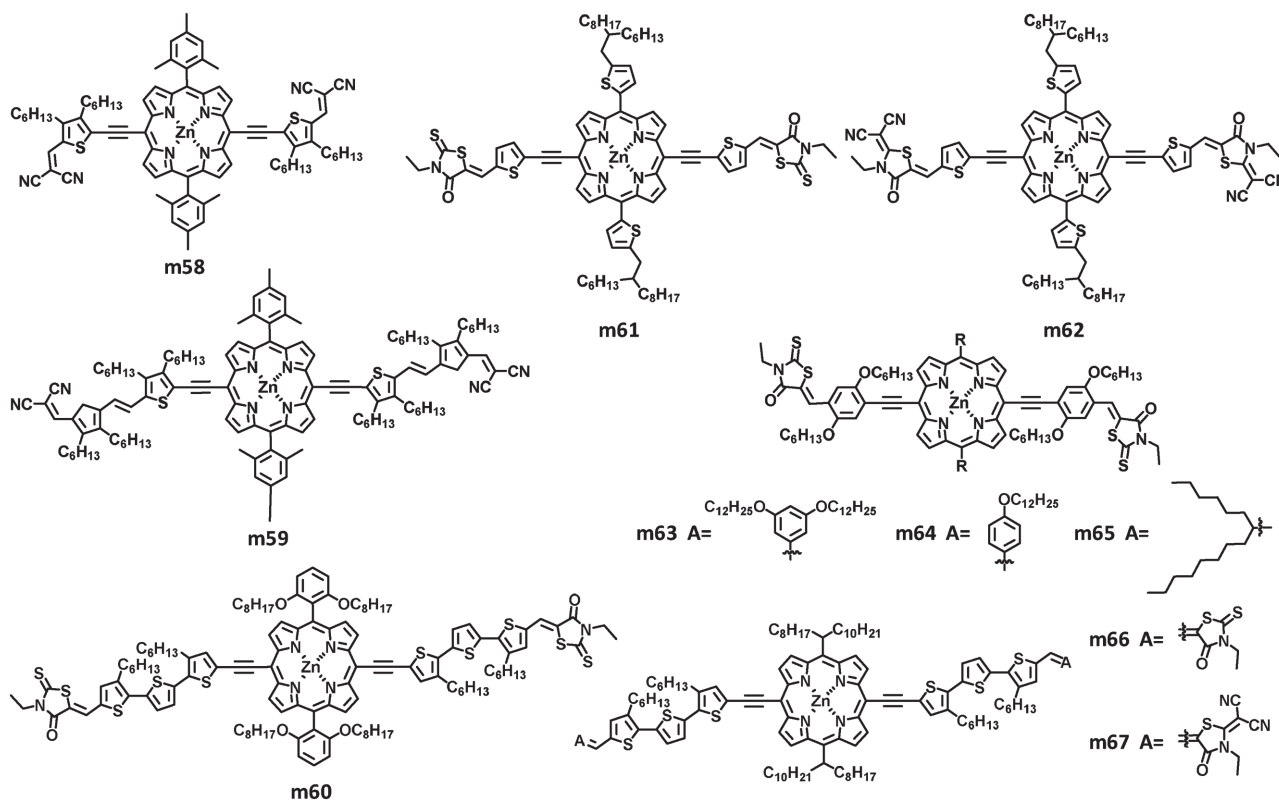

Figure 5. Chemical structures of porphyrin-containing small molecules of **m58**–**m67**.

exhibited a PCE of 8.02% because of favorable absorption and packing behavior.[57] Min et al. reported a DTN-based molecule named UU07 (**m98**) whose performance was extremely sensitive to the solvent vapor annealing process using chloroform as solvent. Films treated with chloroform vapor for 90 s exhibited the best performance with a PCE of over 6.0%.[58] Recently, Domínguez et al. presented two planar SMs RD5 (**m99**) and RD6 (**m100**) based on cyclopentadithiophene derivative (CPDT). The RD6 and RD5 optimized devices exhibited PCE values of 3.72% and 2.77%, respectively. As declared, the absence of one hexyl chain in RD6 contributed to a satisfactory film nanomorphology because of improved mixing, which led to a small domain size that facilitated satisfactory charge balance transport and collection to the contacts.[59]

Figure 6 shows the chemical structures of **m68–m100**. With a D1–A–D2–A–D1-type molecular structure, OSCs based on DTS-containing small molecule showed an impressive PCE of 9.02%.[60] However, OSCs based on DTS-containing A–π–D–π–A small molecule performed a slightly lower PCE of 8.02% because of the low J_{SC} and FF of devices (as shown in **Table 4**).[57] Despite the effect of device engineering, methods should enhance the absorption and charge carrier mobility for DTS-containing A–π–D–π–A small molecules.

2.5. Other Small Molecules

Aside from the popular and widely investigated donors, efforts have been made to apply other functional groups as donor moieties in A–π–D–π–A SMs. Bai et al. first introduced 4,4,9,9-tetrakis(4-hexylphenyl)-indaceno[1,2-b:5,6-b′]dithiophene as the central building block to A–π–D–π–A small molecules
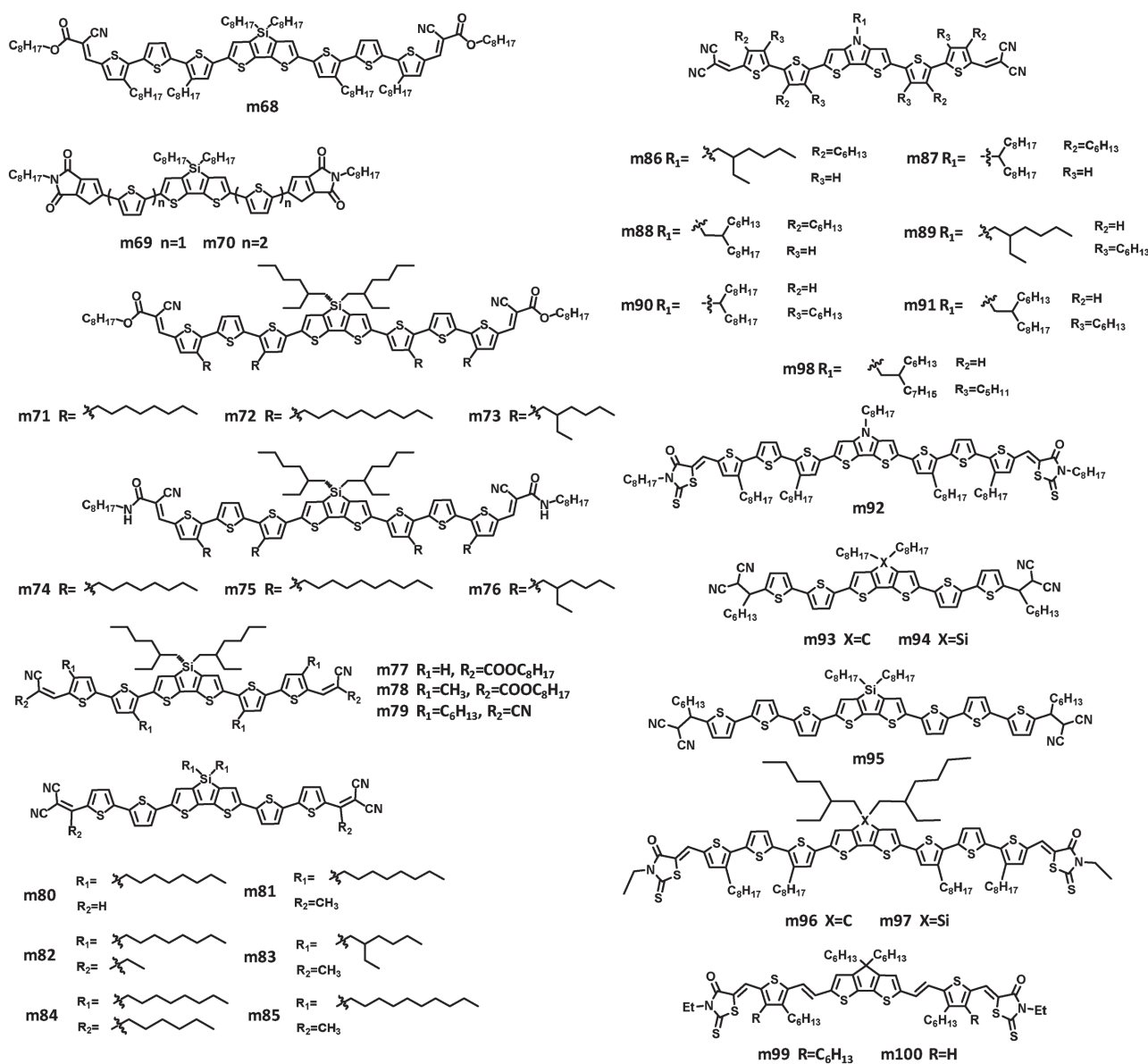

Figure 6. Chemical structures of **m68–m100**.

**ADVANCED
SCIENCE NEWS**
www.advancedsciencenews.com

**Macromolecular
Rapid Communications**
www.mrc-journal.de

Table 4. Photophysical and device performance parameters of **m68**–**m100**.

SM	Acceptor	E_g^{opt} [eV]	HOMO [eV]	LUMO [eV]	μ_h [cm^2 V^{-1} s^{-1}]	V_{OC} [V]	J_{SC} [mA cm^{-2}]	FF [%]	PCE [%]	References
m68	PC$_{61}$BM	1.73	−4.95	−3.26	1.80×10^{-4}	0.80	11.51	64.0	5.84	[49]
m69	PC$_{61}$BM	1.92	−5.55	−3.44	–	0.89	2.56	33.4	0.76	[50]
m70	PC$_{61}$BM	1.87	−5.52	−3.57	–	0.88	2.59	32.9	0.75	[50]
m71	PC$_{61}$BM	1.76	−5.28	−3.52	–	0.82	9.79	54.0	4.31	[51]
m72	PC$_{61}$BM	1.75	−5.27	−3.52	–	0.82	9.30	57.0	4.31	[51]
m73	PC$_{61}$BM	1.82	−5.47	−3.65	–	0.94	7.75	41.0	3.00	[51]
m74	PC$_{61}$BM	1.85	−5.35	−3.50	–	0.87	7.94	47.0	3.22	[51]
m75	PC$_{61}$BM	1.81	−5.34	−3.53	–	0.86	8.38	52.0	3.75	[51]
m76	PC$_{61}$BM	1.92	−5.02	−3.10	–	0.64	1.25	26.0	0.21	[51]
m77	PC$_{61}$BM	1.84	−5.17	−3.37	–	0.92	6.37	56.0	3.27	[52]
m78	PC$_{61}$BM	1.75	−5.08	−3.31	–	0.89	6.61	49.0	2.88	[52]
m79	PC$_{61}$BM	1.72	−5.12	−3.45	–	0.92	8.73	48.0	3.81	[52]
m80	PC$_{71}$BM	1.65	−5.32	−3.45	2.12×10^{-4}	0.84	4.00	43.1	1.50	[53]
m81	PC$_{71}$BM	1.60	−5.26	−3.34	1.01×10^{-3}	0.90	10.00	68.8	6.20	[53]
m82	PC$_{71}$BM	1.62	−5.32	−3.39	6.68×10^{-5}	0.90	8.80	52.9	4.20	[53]
m83	PC$_{71}$BM	1.71	−5.30	−3.35	4.45×10^{-7}	0.90	7.20	62.8	4.10	[53]
m84	PC$_{71}$BM	1.64	−5.32	−3.39	5.30×10^{-4}	0.95	5.80	35.0	1.90	[53]
m85	PC$_{71}$BM	1.64	−5.32	−3.37	6.33×10^{-4}	0.90	8.30	62.1	4.60	[53]
m86	PC$_{61}$BM	1.61	−5.28	−3.68	0.90×10^{-4}	0.83	8.80	66.0	4.80	[54]
m87	PC$_{61}$BM	1.61	−5.28	−3.64	0.60×10^{-4}	0.81	10.50	66.0	5.60	[54]
m88	PC$_{61}$BM	1.60	−5.27	−3.67	1.10×10^{-4}	0.84	8.40	66.0	4.60	[54]
m89	PC$_{61}$BM	1.58	−5.30	−3.75	1.20×10^{-4}	0.83	8.20	65.0	4.40	[54]
m90	PC$_{61}$BM	1.59	−5.31	−3.75	1.10×10^{-4}	0.84	11.40	63.0	6.10	[54]
m91	PC$_{61}$BM	1.58	−5.30	−3.73	1.60×10^{-4}	0.84	10.10	72.0	6.10	[54]
m92	PC$_{71}$BM	1.49	−4.74	−3.26	2.86×10^{-4}	0.67	8.22	55.0	3.03	[55]
m93	PC$_{71}$BM	1.60	−5.29	−3.34	8.26×10^{-5}	0.90	6.85	34.7	2.14	[56]
m94	PC$_{71}$BM	1.57	−5.30	−3.35	3.45×10^{-5}	0.95	6.82	31.8	2.06	[56]
m95	PC$_{71}$BM	1.65	−5.16	−3.27	5.40×10^{-5}	0.78	6.89	38.9	2.09	[56]
m96	PC$_{71}$BM	1.71	−4.93	−3.27	7.50×10^{-5}	0.85	2.74	30.0	0.71	[57]
m97	PC$_{71}$BM	1.66	−4.94	−3.28	4.35×10^{-4}	0.82	13.67	69.0	8.02	[57]
m99	PC$_{71}$BM	1.71	−5.31	−3.60	1.60×10^{-4}	0.81	6.25	54.0	2.77	[59]
m100	PC$_{71}$BM	1.71	−5.32	−3.61	6.20×10^{-6}	0.85	8.25	53.0	3.72	[59]

with bithiophene or terthiophene as π-bridges, alkyl cyanoacetate or rhodanine as end-capped groups and synthesized compounds C-IDT2T (**m101**), R-IDT2T (**m102**), C-IDT3T (**m103**), and R-IDT3T (**m104**). Solar cells based on SMs/PC$_{71}$BM blends showed PCEs of 2.4–5.32%.[61] Tan et al. designed and synthesized a A–π–D–π–A-type small molecule PTZ2 (**m105**) with phenothiazine as the central building block and dicyanovinyl as end-group. A narrower band gap and wider response to the solar spectrum than its D–π–A counterpart were observed; therefore, an improved PCE of 3.25% was obtained.[62] Based on PTZ2, Cheng et al. reported a small molecule POZ6 (**m106**) using phenoxazine as donor group, which exhibited a PCE of 5.6% blended with PC$_{71}$BM.[63] Ni et al. presented a pair of SMs denoted as DCAO3TF (**m107**) and DCAO3TCz (**m108**),

with fluorene and carbazole as central building blocks, respectively. Devices based on SMs/PC$_{61}$BM demonstrated PCEs of 2.38% and 3.63%, respectively.[64] Feng et al. designed two SMs DR2TDTCz (**m109**) containing dithieno[3,2b;6,7-b]carbazole (DTCz) and DR3TCz (**m110**) containing carbazole and two unfused thiophene rings. DR2TDTCz-based solar cells exhibited an impressive PCE of 7.03% owing to improved solar light absorption and more favorable molecular packing compared with DR3TCz.[65] Li et al. designed and synthesized a novel small molecule with carbazole as donor and thiobarbituric acid as acceptor, namely, DTB3TCz (**m111**), which showed deep HOMO and LUMO energy levels and an optimized device PCE of 5.26%.[66] Wang et al. reported three SMs with piro[cyclopenta[1,2-b:5,4-b']dithiophene-4,9'-fluorene] (STF) as

**ADVANCED
SCIENCE NEWS**
www.advancedsciencenews.com

**Macromolecular
Rapid Communications**
www.mrc-journal.de

the central donor unit, terthiophene as the π-conjugated bridge, and indenedione (STFYT, **m112**), 3-ethylrhodanine (STFRDN, **m113**), or 2-(1,1dicyanomethylene)rhodanine (STFRCN, **m114**) as the acceptor unit. These three molecules exhibited desirable physicochemical features: wide absorption bands and high molar absorption coefficients and relatively low HOMO levels. Optimized devices based on SMs/PC$_{71}$BM demonstrated PCE values of 6.68%, 3.30%, and 4.33%, respectively.[67]

Poly(3,4-ethylenedioxythiophene) is a widely used semiconducting polymer in OSCs and functions as a hole transporting material along with poly(sodium-p-styrenesulfonate) (PSS).[68] In 2013, Montcada et al. synthesized a A–π–D–π–A SM using 3,4-ethylenedioxythiophene (EDOT) as the donor group and DCV as the end-capped acceptor, namely, smL01 (**m115**), which yielded a PCE of 3.75% with a high V_{OC} of 1.01 V and an FF of 63.05%.[69] The same group presented a family of SMs smL02–06 (**m116–m120**). Various π-conjugated bridges and end-capped group 3-ethylrhodanine were introduced into smL01, and smL06 showed the highest PCE of 4.9% with an outstanding J_{SC} of 12 mA cm^{-2} owing to the highest IPCE value.[70] To determine the origin of high V_{OC}s of these molecules, Tuladhar et al. analyzed the V_{OC} losses using electroluminescence and external quantum efficiency (EQE) measurements and the relationship between light absorption and emission. The remarkably small breadth of the absorption edge (less than 0.01 eV) and weak nonradiative recombination accounted for the subtle voltage losses.[71] Antwi et al. reported three SM-containing EDOT as core unit with indenedione (DIN-2TE, **m121**), 3-ethylrhodanine (DRH-2TE, **m122**), and ethyl 2-cyanoacetate (DECA-2TE, **m123**) as end-capped units. Solar cells based on DRH-2TE/PC$_{71}$BM exhibited a remarkable PCE of 1.36%.[72]

Naphthodithiophene (NDT) is a popular group that is used as donor moiety in semiconducting D–A copolymers and SMs.[73] Our group first applied the NDT unit into a pair of 2D A–π–D–π–A small molecules containing alkylthienyl or alkylphenyl side chains, denoted as NDTT-CNCOO (**m124**) and NDTPCNCOO (**m125**), respectively. Compared with NDTT-CNCOO, NDTP-CNCOO-based BHJ solar cells exhibited higher FF and J_{SC} values, and thus, a higher PCE of 7.20% with an active layer thickness of 300 nm, which benefitted from highly ordered structures, excellent charge transport property, and good film formation capability. The PCEs of OSCs were all above 6.0% with a film thickness of 200–400 nm, which indicated that a 2D-conjugated NDT core is an effective building block for designing novel and highly efficient small molecules applied in thick-film BHJ solar cells.[74] Chemical structures of **m101–m125** are shown in **Figure 7**.

Recently, two oligomeric molecules, BDTTNTTR and BDTSTNTTR, with A1–π–A2–π–D–π–A2–π–A1-type structure, were reported by Wan et al. By introducing the electron deficient naphtho[1,2-c:5,6-c']bis[1,2,5]thiadiazole (NT) group as the second acceptor block and extending the π-conjugation length of the whole molecular backbone, as well as applying the halogen-free solvent carbon disulfide, remarkable PCEs of 10.02% and 11.53% for BDTTNTTR-based and BDTSTNTTR-based solar cells were achieved, respectively.[2c] PCE of over 12% for small molecule-based tandem solar cells was realized by Li et al. by using BDT-containing SM DR3TSBDT (**m7**) and

porphyrin-containing A-D-A-type SM DPPEZnP-TBO as donor materials for two active layers.[75]

3. Small Molecule: Nonfullerene Acceptor OSCs

Fullerene-free organic solar cells have recently attracted considerable attention because of their excellent performance.[76] With nonfullerene small molecule acceptors, polymer solar cells have yielded PCEs of over 12%.[2a,77] Thus, researchers have applied electron-donating small molecules to fabricate fullerene-free OSCs. With D1–A–D2–A–D1-type small molecule 7,7'-(4,4-bis(2-ethylhexyl)-4H-silolo[3,2-b:4,5-b']dithiophene-2,6diyl)bis(6-fluoro-4-(5'-hexyl-[2,2'-bithiophen]-5-yl)benzo[c][1,2,5]thiadiazole) (p-DTS(FBTTh$_2$)$_2$) as donor and (2E,2'E)-3,3'-(2,5-dimethoxy-1,4-phenylene)bis(2-(5-(4-(N-(2-ethylhexyl)1,8-naphthalimide)-yl)thiophen-2-yl)acrylonitrile) (NIDCS-MO) as acceptor, Kwon et al. fabricated all small molecule fullerene-free OSCs, and a PCE of 5.30% with a V_{OC} of 0.85 V, a J_{SC} of 9.62 mA cm^{-2}, and an FF of 64%.[78] Badgujar et al. reported an SM (5Z,50Z)-5,50-(((4,40,400,8,80,800-hexakis(5-(2-ethylhexyl)-thiophen-2-yl)-[2,20:60,200-terbenzo[1,2-b:4,5-b0]dithiophene]-6,600-diyl)bis(3,300-dioctyl-[2,20:50,200-terthiophene]-500,5-diyl))bis(methanylylidene))bis(3-ethyl-2-thioxothiazolidin-4-one) named BDT3TR with A–π–D–π–A structure. With nonfullerene small molecule n-octyl-indacenodithiophene-bis(2,1,3-benzothiadiazole)-bis(3-ethylrhodanine) (O-IDTBR) as the acceptor, the devices showed an excellent PCE exceeding 7%.[79] Recently, Yang et al. designed and synthesized an A–D–A small molecule DRTB-T and fabricated solar cells with IC-C61DT-IC as acceptor. After solvent vapor annealing, an impressive PCE of 9.08% with a V_{OC} of 0.98 V, a J_{SC} of 14.25 mA cm^{-2}, and an FF of 65% were achieved.[80] With a D–A structured medium bandgap, small molecule H11 with BDTT as central donor unit, and fluorobenzotriazole as acceptor unit, Bin et al. updated the performance of small molecule fullerene-free OSCs with a high PCE of 9.73%.[81] As seen in refs. [80] and [81], to supply the red-shifted absorption band of nonfullerene acceptors, electron-donating small molecules for fullerene-free OSCs need to have a larger optical band gap (>1.8 eV) than that in fullerene-containing OSCs. Owing to their unique chemical structure, A–π–D–π–A small molecules usually have medium or small band gaps (**Tables** 1–**5**). Thus, strategies to enlarge the optical band gaps of A–π–D–π–A small molecules should be explored. With fine-tuned modification and carefully selected acceptor material, A–π–D–π–A small molecules could show extraordinary results in small molecule fullerene-free OSCs in the future.

4. Statistical Analysis

We conducted the statistical analysis of the J_{SC}s versus optical band gaps of all reviewed A–π–D–π–A small molecules (see **Figure 8**a). For SMs with the band gap in the range of 1.4–1.9 eV, J_{SC}s of over 12 mA cm^{-2} can be achieved, and with a band gap of 1.6–1.8 eV, J_{SC}s can reach nearly 16 mA cm^{-2}. However, a narrow band gap does not mean a high J_{SC}. A statistical summary of the relationship between V_{oc} and optical band gap and the relationship between V_{OC} and the difference of the LOMO

ADVANCED
SCIENCE NEWS
www.advancedsciencenews.com

Macromolecular
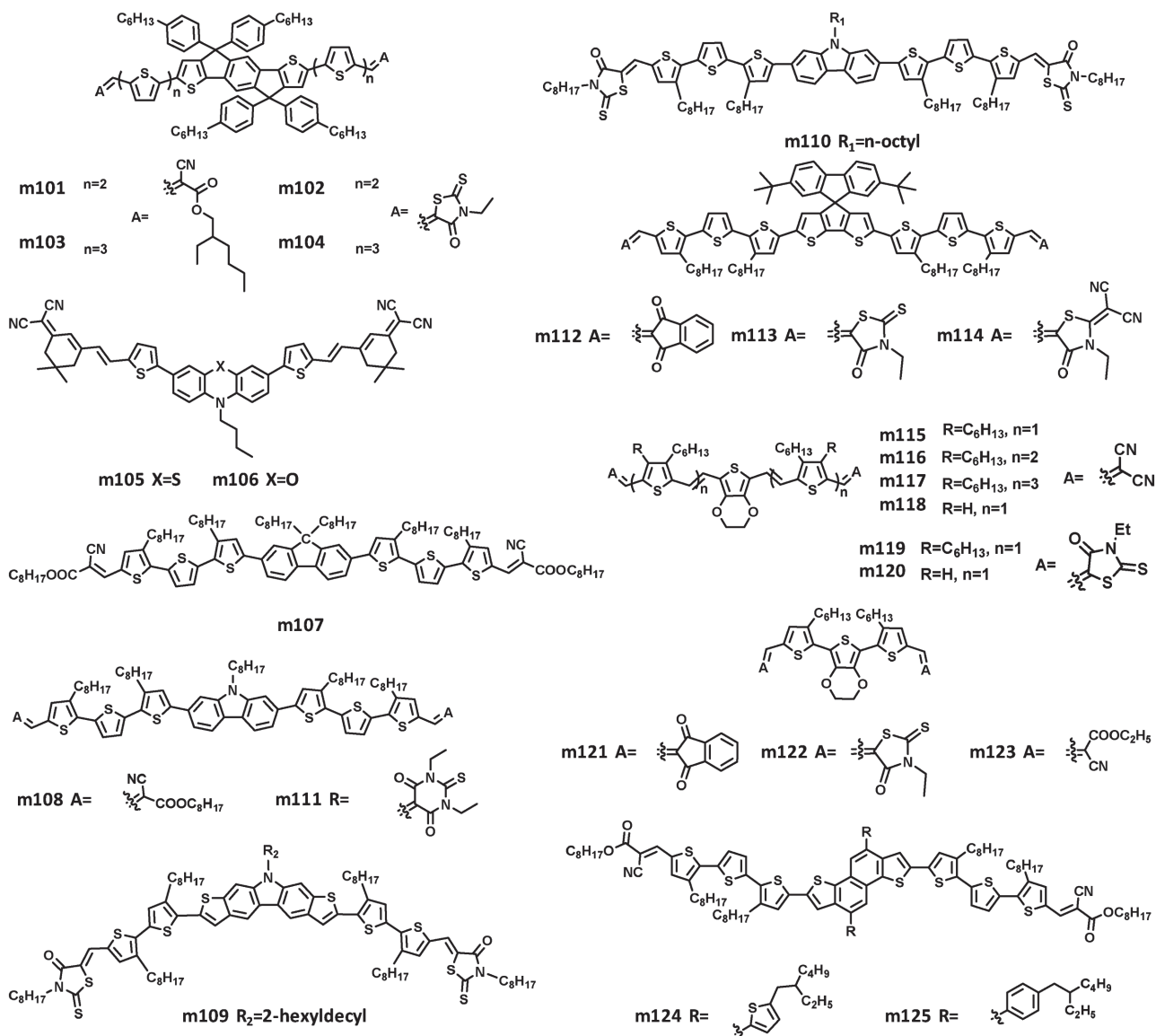Rapid Communications
www.mrc-journal.de

Figure 7. Chemical structures of **m101–m125**.

level of acceptor and the HOMO level of donor was performed (as shown in Figure 8b,c). The larger the band gap or the difference is, the higher the V_{OC} of OSCs. The V_{OC} of BHJ OSCs is determined by the difference between the LUMO of electron-withdrawing materials and the HOMO of electron-donating materials.[82] However, because V_{OC} is influenced by many factors, such as recombination,[83] quasi-Fermi levels,[3b] DOS distribution,[3a] energetic disorders,[3d] charge transfer state,[84] and work functions of electrodes,[85] these relationships are not likely to be a linear function. Actually, many SMs with HOMO levels deeper than −5.0 eV can yield high V_{OC} values over 0.9 V, with optimized device engineering. In addition to designing SMs with deep HOMO energy levels, reducing the energy losses in devices can be an effective method to obtain high V_{OC} values and hence, high PCEs. Moreover, the relationship of hole mobility values of D–A blend films and FF of OSCs is shown in Figure 8d. Interestingly, achieving high FF with high

hole mobility values is easy, whereas remarkable FFs were well obtained by blend films with low mobility values of below 1 × 10^{-4} cm^2 V^{-1} s^{-1}. High FFs can be realized by films with a hole mobility ranging from 10^{-5}–10^{-4} cm^2 V^{-1} s^{-1}.

Statistical analysis of the PCEs of OSCs versus optical band gaps of small molecules was performed (see **Figure 9**a). For SMs with the band gap in the range of 1.4–1.9 eV, devices can exhibit PCEs over 6%. However, the most impressive performances are achieved by SMs with an optical band gap of 1.6–1.8 eV, which is consistent with the band gap–J_{SC} relationship. Moreover, the record-breaking efficiencies for both SMs/ PC$_{61}$BM and SMs/PC$_{71}$BM systems contain a SM with a band gap of ≈1.7 eV, which denotes an absorption band edge of ≈730 nm. Figure 9b shows a concentrated and linear distribution of PCE versus J_{SC}. Surely the J_{SC} plays the most important role in the performance of OSCs, and a high J_{SC} promises a high PCE. The PCE–V_{OC} relationship is shown in Figure 9c. The

Table 5. Photophysical and device performance parameters of **m101–m125**.

SM	Acceptor	E_g^{opt} [eV]	HOMO [eV]	LUMO [eV]	μ_h [cm^2 V^{-1} s^{-1}]	V_{OC} [V]	J_{SC} [mA cm^{-2}]	FF [%]	PCE [%]	References
m101	PC$_{71}$BM	1.92	−5.22	−3.28	7.50×10^{-5}	0.88	7.98	33.1	2.53	[61]
m102	PC$_{71}$BM	1.86	−5.21	−3.27	5.00×10^{-5}	0.93	10.11	44.5	4.38	[61]
m103	PC$_{71}$BM	1.90	−5.18	−3.29	1.70×10^{-4}	0.91	10.52	49.6	5.00	[61]
m104	PC$_{71}$BM	1.88	−5.19	−3.27	3.00×10^{-4}	0.90	11.50	49.0	5.32	[61]
m105	PC$_{71}$BM	1.82	−5.51	−3.69	–	0.97	10.30	32.5	3.25	[62]
m106	PC$_{71}$BM	1.65	−5.31	−3.66	2.24×10^{-4}	0.86	13.10	49.6	5.60	[63]
m107	PC$_{61}$BM	2.01	−5.32	−3.23	1.12×10^{-4}	1.07	4.54	49.0	2.38	[64]
m108	PC$_{61}$BM	1.92	−5.14	−3.21	1.62×10^{-4}	0.97	6.15	61.0	3.63	[64]
m109	PC$_{71}$BM	1.74	−5.05	−3.31	3.78×10^{-5}	0.90	10.34	75.0	7.03	[65]
m110	PC$_{71}$BM	1.80	−5.08	−3.28	9.10×10^{-5}	0.94	8.02	54.0	4.08	[65]
m111	PC$_{71}$BM	1.61	−5.16	−3.56	1.96×10^{-4}	0.91	11.80	49.0	5.26	[66]
m112	PC$_{71}$BM	1.61	−5.38	−3.71	1.57×10^{-4}	0.79	12.88	65.8	6.68	[67]
m113	PC$_{71}$BM	1.71	−5.25	−3.61	3.15×10^{-5}	0.87	7.21	52.5	3.30	[67]
m114	PC$_{71}$BM	1.57	−5.15	−3.68	1.26×10^{-4}	0.88	10.08	48.9	4.33	[67]
m115	PC$_{71}$BM	1.87	−5.60	−3.73	1.20×10^{-6}	1.01	5.89	63.0	3.75	[69]
m116	PC$_{71}$BM	1.76	−5.26	−3.50	1.10×10^{-5}	0.61	3.78	66.43	1.50	[70]
m117	PC$_{71}$BM	1.80	−5.03	−3.23	2.80×10^{-5}	0.56	2.70	52.6	0.80	[70]
m118	PC$_{71}$BM	1.88	−5.62	−3.74	5.90×10^{-7}	0.92	2.50	45.4	1.10	[70]
m119	PC$_{71}$BM	1.82	−5.41	−3.59	1.80×10^{-4}	0.91	4.70	34.9	1.50	[70]
m120	PC$_{71}$BM	1.84	−5.41	−3.57	1.40×10^{-5}	0.89	11.98	45.7	4.90	[70]
m121	PC$_{71}$BM	1.57	−5.49	−3.18	–	–	–	–	–	[72]
m122	PC$_{71}$BM	1.71	−5.13	−3.16	–	0.68	5.60	35.0	1.36	[72]
m123	PC$_{71}$BM	1.82	−5.46	−3.30	–	0.90	2.99	39.0	1.05	[72]
m124	PC$_{71}$BM	1.85	−5.16	−3.48	2.44×10^{-4}	0.91	7.40	69.9	4.71	[74]
m125	PC$_{71}$BM	1.88	−5.18	−3.45	3.81×10^{-4}	0.94	10.77	71.1	7.20	[74]

highest PCEs were achieved by OSCs with V_{OC}s of ≈0.95 V, and an obvious linear relationship of the highest PCE versus V_{OC} can be found when V_{OC} values are below 0.95 V. Examples of OSCs with V_{OC}s over 1 V exist, but the efficiencies are unsatisfying. Statistical summary of PCEs versus FF of SM-based solar cells was conducted, as shown in Figure 9d. Similar to J_{SC}, the higher the FF is, the better the performance of OSCs. However, without remarkable J_{SC}, even with high FFs of over 60%, obtaining a high PCE is difficult. PCE of OSC is mainly attributed to two factors of electronic properties of molecules and morphology of the active layer. These two factors influence light absorption, charge generation, charge separation, and charge transport processes throughout, and dominate the values of V_{OC}, J_{SC}, and FF of OSCs. Achieving high PCEs with one single high value of the three parameters is difficult.

5. Summary and Outlook

Over 100 electron-donating A–π–D–π–A-type small molecules for solution-processed organic solar cells have been reviewed. These SMs with PCEs ranging from less than 1% to over 11%

contributed dramatically to the development of organic photovoltaics. Further statistical analysis of data listed in Tables 1–5 could provide us with inspiration to design small molecules with improved performances.

$$PCE = \frac{V_{OC} \times J_{SC} \times FF}{P_{in}} \qquad (1)$$

PCE of BHJ solar cells directly depends on the three device parameters, namely, V_{OC}, J_{SC}, and FF, as shown in Equation (1), in which P_{in} is the incident solar power.[86] With a certain FF value, researchers are seeking methods of obtaining both high V_{OC}s and high J_{SC}s. Up to now several practical challenges need to be resolved, because improved performances of these issues need to be achieved

(1) Balance between V_{OC} and J_{SC}. When using PC$_{61}$BM or PC$_{71}$BM as electron-withdrawing material, a deeper HOMO level for electron-donating SM may contribute to a higher V_{OC}. However, to provide enough driving force for electron to transport from donor to acceptor, the LUMO level of the donor material needs to be slightly higher than the LUMO level of the acceptor material. Therefore, SMs with a deeper HOMO
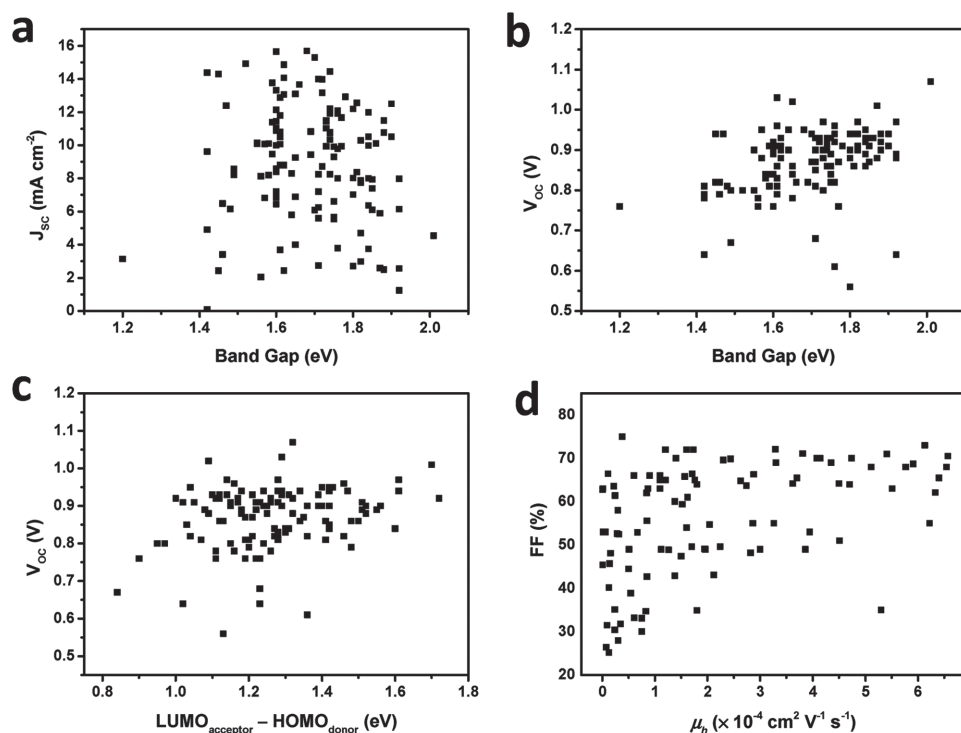
**ADVANCED
SCIENCE NEWS**
www.advancedsciencenews.com

**Macromolecular
Rapid Communications**
www.mrc-journal.de

Figure 8. a) Statistical summary of J_{SC} versus optical band gaps of SMs. b) Statistical summary of V_{OC} versus optical band gaps of SMs. c) Statistical summary of V_{OC} versus the difference between the LOMO level of acceptor and the HOMO level of donor. d) Statistical summary of FF versus hole mobility values of SM/fullerene blends (data from Tables 1–5).
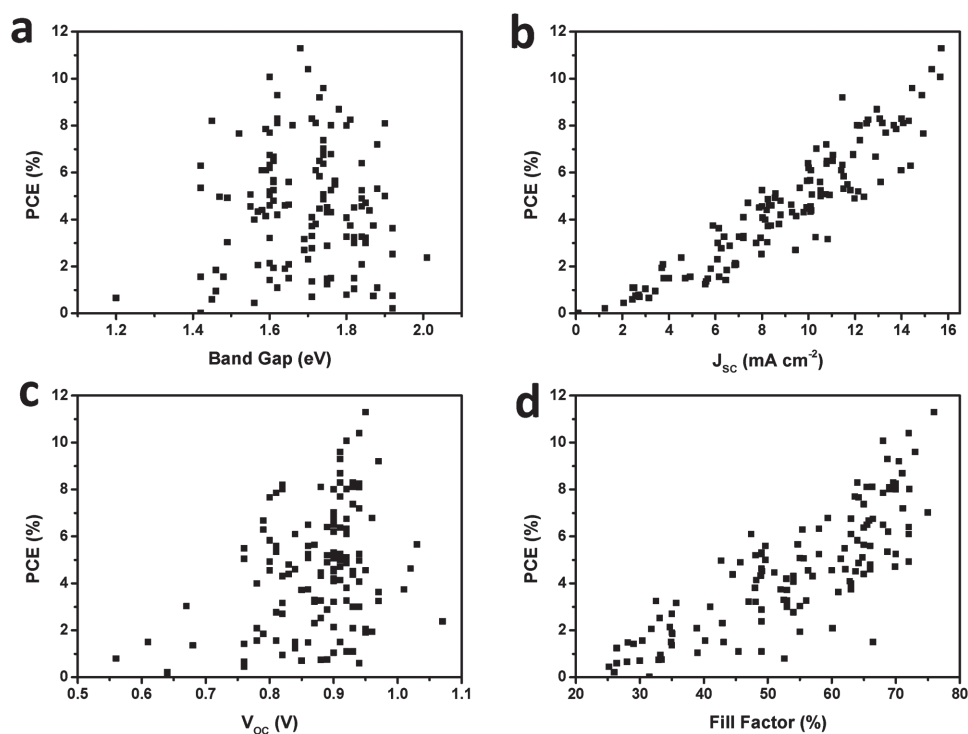

Figure 9. a) Statistical summary of PCEs versus optical band gaps of SMs. b) Statistical summary of PCEs versus J_{SC}s of SM-based solar cells. c) Statistical summary of PCEs versus V_{OC}s of SM-based solar cells. d) Statistical summary of PCEs versus FF of SM-based solar cells (data from Tables 1–5).

**ADVANCED
SCIENCE NEWS**
www.advancedsciencenews.com

**Macromolecular
Rapid Communications**
www.mrc-journal.de

level usually perform a larger optical band gap, which means a narrower and a more blue-shifted absorption band. J_{SC} mainly depends on the ability of absorbing solar light and on the EQE of the active layer. We can conclude that achieving high V_{OC} and J_{SC} in one certain BHJ OSCs system is challenging. Thus, a controllable balance between the optical band gaps and electrochemical HOMO levels for electron-donating small molecules is needed. In the case of fullerene-free OSCs, because of controllable band gaps and energy levels of electron-withdrawing materials, plenty of room is provided for electron-donating small molecules to achieve supplementary light absorption and good charge transport properties.

(2) Decent morphology and domain purity. The three parameters of OSCs are not only dominated by the properties of SMs but also affected by the morphology of active layers and device structures.[87] Suitable domain size and domain purity are greatly needed for high excitation dissociation efficiency and charge carrier mobility. Bicontinuous and favorable phase separation, including vertical phase separation, and efficient interlayers play important roles in collecting and transporting charges. When it comes to D–A phase separation, a balance between crystalizing speed and phase separating speed needs to be noted. The donor and acceptor materials should perform proper crystallinity and miscibility, which can be evaluated by the π–π interaction and surface energy of the molecules. For fullerene-free OSCs, finding an appropriate acceptor molecule to cooperate with the donor molecule is important.

(3) Good stability and homogeneity. Owing to high crystallinity, SM-based OSCs show poor homogeneity and stability compared with polymer-based OSCs. Equal performances obtained under the same fabricating conditions are unsure, and the quasiequilibrium packing state is likely to overage easily. Only a few studies have mentioned stability and homogeneity; thus, more studies are needed to overcome these issues.

By carefully selecting donor and acceptor moieties and π-conjugated bridges, one can design SMs with appropriate band gaps, energy levels, and planarity. Applying fullerene derivatives as electron-withdrawing materials, electron-donating SMs exhibited better performance with an optical band gap of 1.6–1.8 eV. With proper HOMO level and device engineering, a V_{OC} between 0.9 and 1 V is a good choice for high PCEs. Decreasing the energy loss in active layer can be a better approach to obtain high V_{OC} than deepening the HOMO level. Toward high PCEs over 12%, researchers should find methods of improving the J_{SC} without sacrificing high V_{OC} and FF. With fine structural layouts and chemical and photophysical properties, A–π–D–π–A-type small molecules are now one of the most promising materials for high performance single junction BHJ OSCs.

Acknowledgements

Conflict of Interest

The authors declare no conflict of interest.

Keywords

[1] a) L. Dou, J. You, Z. Hong, Z. Xu, G. Li, R. A. Street, Y. Yang, *Adv. Mater.* **2013**, *25*, 6642; b) F. C. Krebs, N. Espinosa, M. Hösel, R. R. Søndergaard, M. Jørgensen, *Adv. Mater.* **2014**, *26*, 29; c) L. Lu, M. A. Kelly, W. You, L. Yu, *Nat. Photonics* **2015**, *9*, 491.

[2] a) W. Zhao, S. Li, H. Yao, S. Zhang, Y. Zhang, B. Yang, J. Hou, *J. Am. Chem. Soc.* **2017**, *139*, 7148; b) D. Deng, Y. Zhang, J. Zhang, Z. Wang, L. Zhu, J. Fang, B. Xia, Z. Wang, K. Lu, W. Ma, Z. Wei, *Nat. Commun.* **2016**, *7*, 13740; c) J. Wan, X. Xu, G. Zhang, Y. Li, K. Feng, Q. Peng, *Energy Environ. Sci.* **2017**, *10*, 1739.

[3] a) G. Garcia-Belmonte, J. Bisquert, *Appl. Phys. Lett.* **2010**, *96*, 113301; b) J. C. Blakesley, D. Neher, *Phys. Rev. B* **2011**, *84*, 075210; c) T. S. Ripolles, A. Guerrero, G. Garcia-Belmonte, *Appl. Phys. Lett.* **2013**, *103*, 243306; d) S. D. Collins, C. M. Proctor, N. A. Ran, T.-Q. Nguyen, *Adv. Energy Mater.* **2016**, *6*, 1501721.

[4] J. Roncali, *Chem. Rev.* **1997**, *97*, 173.

[5] a) Y. Lin, Y. Li, X. Zhan, *Chem. Soc. Rev.* **2012**, *41*, 4245; b) Y. Chen, X. Wan, G. Long, *Acc. Chem. Res.* **2013**, *46*, 2645; c) X. Liu, H. Chen, S. Tan, *Renewable Sustainable Energy Rev.* **2015**, *52*, 1527; d) S. D. Collins, N. A. Ran, M. C. Heiber, T. Q. Nguyen, *Adv. Energy Mater.* **2017**, *7*, 1602242; e) A. Tang, C. Zhan, J. Yao, E. Zhou, *Adv. Mater.* **2017**, *29*, 1600013.

[6] a) S. Loser, C. J. Bruns, H. Miyauchi, R. P. Ortiz, A. Facchetti, S. I. Stupp, T. J. Marks, *J. Am. Chem. Soc.* **2011**, *133*, 8142; b) J. Huang, C. Zhan, X. Zhang, Y. Zhao, Z. Lu, H. Jia, B. Jiang, J. Ye, S. Zhang, A. Tang, Y. Liu, Q. Pei, J. Yao, *ACS Appl. Mater. Interfaces* **2013**, *5*, 2033; c) Y. Lin, L. Ma, Y. Li, Y. Liu, D. Zhu, X. Zhan, *Adv. Energy Mater.* **2013**, *3*, 1166; d) Y. J. Kim, J. Y. Baek, J.-j. Ha, D. S. Chung, S.-K. Kwon, C. E. Park, Y.-H. Kim, *J. Mater. Chem. C* **2014**, *2*, 4937; e) H. Qin, L. Li, F. Guo, S. Su, J. Peng, Y. Cao, X. Peng, *Energy Environ. Sci.* **2014**, *7*, 1397.

[7] a) O. P. Lee, A. T. Yiu, P. M. Beaujuge, C. H. Woo, T. W. Holcombe, J. E. Millstone, J. D. Douglas, M. S. Chen, J. M. J. Fréchet, *Adv. Mater.* **2011**, *23*, 5359; b) J. Hatano, N. Obata, S. Yamaguchi, T. Yasuda, Y. Matsuo, *J. Mater. Chem.* **2012**, *22*, 19258; c) R. B. Zerdan, N. T. Shewmon, Y. Zhu, J. P. Mudrick, K. J. Chesney, J. Xue, R. K. Castellano, *Adv. Funct. Mater.* **2014**, *24*, 5993; d) S. X. Sun, Y. Huo, M. M. Li, X. Hu, H. J. Zhang, Y. W. Zhang, Y. D. Zhang, X. L. Chen, Z. F. Shi, X. Gong, Y. Chen, H. L. Zhang, *ACS Appl. Mater. Interfaces* **2015**, *7*, 19914; e) O. Vybornyi, Y. Jiang, F. Baert, D. Demeter, J. Roncali, P. Blanchard, C. Cabanetos, *Dyes Pigm.* **2015**, *115*, 17.

[8] a) X. Wan, Y. Liu, F. Wang, J. Zhou, G. Long, Y. Chen, *Org. Electron.* **2013**, *14*, 1562; b) W. Yan, Q. Zhang, Q. Qin, S. Ye, Y. Lin, Z. Liu,

Z. Bian, Y. Chen, C. Huang, *Dyes Pigm.* **2015**, *121*, 99; c) H. Zhang, Y. Liu, Y. Sun, M. Li, B. Kan, X. Ke, Q. Zhang, X. Wan, Y. Chen, *Chem. Commun.* **2016**, *53*, 451; d) Y. Zhao, X. Zhou, K. Wu, H. Wang, S. Qu, F. He, C. Yang, *Dyes Pigm.* **2016**, *130*, 282; e) Z. Zhang, Z. Zhou, Q. Hu, F. Liu, T. P. Russell, X. Zhu, *ACS Appl. Mater. Interfaces* **2017**, *9*, 6213.

[9] a) Y. Sun, G. C. Welch, W. L. Leong, C. J. Takacs, G. C. Bazan, A. J. Heeger, *Nat. Mater.* **2011**, *11*, 44; b) P. Dutta, J. Kim, S. H. Eom, W. H. Lee, I. N. Kang, S. H. Lee, *ACS Appl. Mater. Interfaces* **2012**, *4*, 6669; c) J. A. Love, S. D. Collins, I. Nagao, S. Mukherjee, H. Ade, G. C. Bazan, T. Q. Nguyen, *Adv. Mater.* **2014**, *26*, 7308; d) C. V. Kumar, L. Cabau, E. N. Koukaras, G. D. Sharma, E. Palomares, *Org. Electron.* **2015**, *26*, 36; e) A. Tang, C. Zhan, J. Yao, *Adv. Energy Mater.* **2015**, *5*, 1500059; f) J. Sim, K. Do, K. Song, A. Sharma, S. Biswas, G. D. Sharma, J. Ko, *Org. Electron.* **2016**, *30*, 122; g) J. Wolf, M. Babics, K. Wang, Q. Saleem, R.-Z. Liang, M. R. Hansen, P. M. Beaujuge, *Chem. Mater.* **2016**, *28*, 2058.

[10] a) L.-Y. Lin, C.-W. Lu, W.-C. Huang, Y.-H. Chen, H.-W. Lin, K.-T. Wong, *Org. Lett.* **2011**, *13*, 4962; b) P. Li, H. Tong, J. Liu, J. Ding, Z. Xie, L. Wang, *RSC Adv.* **2013**, *3*, 23098; c) S. Xu, Z. Zhou, H. Fan, L. Ren, F. Liu, X. Zhu, T. P. Russell, *J. Mater. Chem. A* **2016**, *4*, 17354; d) Z. Zhou, S. Xu, W. Liu, C. Zhang, Q. Hu, F. Liu, T. P. Russell, X. Zhu, *J. Mater. Chem. A* **2017**, *5*, 3425.

[11] a) S. So, H. Choi, C. Kim, N. Cho, H. M. Ko, J. K. Lee, J. Ko, *Sol. Energy Mater. Sol. Cells* **2011**, *95*, 3433; b) M. Paramasivam, A. Gupta, A. M. Raynor, S. V. Bhosale, K. Bhanuprakash, V. Jayathirtha Rao, *RSC Adv.* **2014**, *4*, 35318; c) L. Wang, L. Yin, C. Ji, Y. Zhang, H. Gao, Y. Li, *Org. Electron.* **2014**, *15*, 1138; d) K. Narayanaswamy, A. Venkateswararao, V. Gupta, S. Chand, S. P. Singh, *Chem. Commun.* **2016**, *52*, 210.

[12] a) M. Li, W. Ni, X. Wan, Q. Zhang, B. Kan, Y. Chen, *J. Mater. Chem. A* **2015**, *3*, 4765; b) W. Ni, X. Wan, M. Li, Y. Wang, Y. Chen, *Chem. Commun.* **2015**, *51*, 4936.

[13] Y. Liu, X. Wan, F. Wang, J. Zhou, G. Long, J. Tian, Y. Chen, *Adv. Mater.* **2011**, *23*, 5387.

[14] J. Zhou, X. Wan, Y. Liu, Y. Zuo, Z. Li, G. He, G. Long, W. Ni, C. Li, X. Su, Y. Chen, *J. Am. Chem. Soc.* **2012**, *134*, 16345.

[15] J. Zhou, Y. Zuo, X. Wan, G. Long, Q. Zhang, W. Ni, Y. Liu, Z. Li, G. He, C. Li, B. Kan, M. Li, Y. Chen, *J. Am. Chem. Soc.* **2013**, *135*, 8484.

[16] B. Kan, Q. Zhang, M. Li, X. Wan, W. Ni, G. Long, Y. Wang, X. Yang, H. Feng, Y. Chen, *J. Am. Chem. Soc.* **2014**, *136*, 15529.

[17] B. Kan, Q. Zhang, F. Liu, X. Wan, Y. Wang, W. Ni, X. Yang, M. Zhang, H. Zhang, T. P. Russell, Y. Chen, *Chem. Mater.* **2015**, *27*, 8414.

[18] C. Cui, X. Guo, J. Min, B. Guo, X. Cheng, M. Zhang, C. J. Brabec, Y. Li, *Adv. Mater.* **2015**, *27*, 7469.

[19] J. Min, C. Cui, T. Heumueller, S. Fladischer, X. Cheng, E. Spiecker, Y. Li, C. J. Brabec, *Adv. Energy Mater.* **2016**, *6*, 1600515.

[20] Z. Du, W. Chen, M. Qiu, Y. Chen, N. Wang, T. Wang, M. Sun, D. Yu, R. Yang, *Phys. Chem. Chem. Phys.* **2015**, *17*, 17391.

[21] Y. Liu, C. C. Chen, Z. Hong, J. Gao, Y. M. Yang, H. Zhou, L. Dou, G. Li, Y. Yang, *Sci. Rep.* **2013**, *3*, 3356.

[22] Q. Fan, M. Li, P. Yang, Y. Liu, M. Xiao, X. Wang, H. Tan, Y. Wang, R. Yang, W. Zhu, *Dyes Pigm.* **2015**, *116*, 13.

[23] C. V. Kumar, L. Cabau, E. N. Koukaras, S. A. Siddiqui, G. D. Sharma, E. Palomares, *Nanoscale* **2015**, *7*, 7692.

[24] D. Deng, Y. Zhang, L. Yuan, C. He, K. Lu, Z. Wei, *Adv. Energy Mater.* **2014**, *4*, 1400538.

[25] D. Deng, Y. Zhang, L. Zhu, J. Zhang, K. Lu, Z. Wei, *Phys. Chem. Chem. Phys.* **2015**, *17*, 8894.

[26] S. Shen, P. Jiang, C. He, J. Zhang, P. Shen, Y. Zhang, Y. Yi, Z. Zhang, Z. Li, Y. Li, *Chem. Mater.* **2013**, *25*, 2274.

[27] A. Tang, C. Zhan, J. Yao, *Chem. Mater.* **2015**, *27*, 4719.

[28] W. Ni, M. Li, X. Wan, H. Feng, B. Kan, Y. Zuo, Y. Chen, *RSC Adv.* **2014**, *4*, 31977.

[29] M. Li, F. Liu, X. Wan, W. Ni, B. Kan, H. Feng, Q. Zhang, X. Yang, Y. Wang, Y. Zhang, Y. Shen, T. P. Russell, Y. Chen, *Adv. Mater.* **2015**, *27*, 6296.

[30] K. Schulze, C. Uhrich, R. Schüppel, K. Leo, M. Pfeiffer, E. Brier, E. Reinold, P. Bäuerle, *Adv. Mater.* **2006**, *18*, 2872.

[31] Y. Liu, X. Wan, F. Wang, J. Zhou, G. Long, J. Tian, J. You, Y. Yang, Y. Chen, *Adv. Energy Mater.* **2011**, *1*, 771.

[32] Z. Li, G. He, X. Wan, Y. Liu, J. Zhou, G. Long, Y. Zuo, M. Zhang, Y. Chen, *Adv. Energy Mater.* **2012**, *2*, 74.

[33] G. He, Z. Li, X. Wan, J. Zhou, G. Long, S. Zhang, M. Zhang, Y. Chen, *J. Mater. Chem. A* **2013**, *1*, 1801.

[34] Q. Zhang, B. Kan, F. Liu, G. Long, X. Wan, X. Chen, Y. Zuo, W. Ni, H. Zhang, M. Li, Z. Hu, F. Huang, Y. Cao, Z. Liang, M. Zhang, T. P. Russell, Y. Chen, *Nat. Photonics* **2014**, *9*, 35.

[35] J. Peng, Y. Chen, X. Wu, Q. Zhang, B. Kan, X. Chen, Y. Chen, J. Huang, Z. Liang, *ACS Appl. Mater. Interfaces* **2015**, *7*, 13137.

[36] G. Long, B. Wu, A. Solanki, X. Yang, B. Kan, X. Liu, D. Wu, Z. Xu, W.-R. Wu, U. S. Jeng, J. Lin, M. Li, Y. Wang, X. Wan, T. C. Sum, Y. Chen, *Adv. Energy Mater.* **2016**, *6*, 1600961.

[37] B. Kan, M. Li, Q. Zhang, F. Liu, X. Wan, Y. Wang, W. Ni, G. Long, X. Yang, H. Feng, Y. Zuo, M. Zhang, F. Huang, Y. Cao, T. P. Russell, Y. Chen, *J. Am. Chem. Soc.* **2015**, *137*, 3886.

[38] G. Long, X. Wan, B. Kan, Y. Liu, G. He, Z. Li, Y. Zhang, Y. Zhang, Q. Zhang, M. Zhang, Y. Chen, *Adv. Energy Mater.* **2013**, *3*, 639.

[39] Q. Zhang, Y. Wang, B. Kan, X. Wan, F. Liu, W. Ni, H. Feng, T. P. Russell, Y. Chen, *Chem. Commun.* **2015**, *51*, 15268.

[40] Y. Zuo, Q. Zhang, X. Wan, M. Li, H. Zhang, C. Li, Y. Chen, *Org. Electron.* **2015**, *19*, 98.

[41] F. Liu, H. Fan, Z. Zhang, X. Zhu, *ACS Appl. Mater. Interfaces* **2016**, *8*, 3661.

[42] J. Kesters, P. Verstappen, M. Kelchtermans, L. Lutsen, D. Vanderzande, W. Maes, *Adv. Energy Mater.* **2015**, *5*, 1500218.

[43] S. Arrechea, A. Molina-Ontoria, A. Aljarilla, P. de la Cruz, F. Langa, L. Echegoyen, *Dyes Pigm.* **2015**, *121*, 109.

[44] C. V. Kumar, L. Cabau, E. N. Koukaras, A. Sharma, G. D. Sharma, E. Palomares, *J. Mater. Chem. A* **2015**, *3*, 16287.

[45] K. Gao, L. Xiao, Y. Kan, B. Yang, J. Peng, Y. Cao, F. Liu, T. P. Russell, X. Peng, *J. Mater. Chem. C* **2016**, *4*, 3843.

[46] H. Wang, L. Xiao, L. Yan, S. Chen, X. Zhu, X. Peng, X. Wang, W.-K. Wong, W.-Y. Wong, *Chem. Sci.* **2016**, *7*, 4301.

[47] L. Xiao, S. Chen, K. Gao, X. Peng, F. Liu, Y. Cao, W. Y. Wong, W. K. Wong, X. Zhu, *ACS Appl. Mater. Interfaces* **2016**, *8*, 30176.

[48] Y. I. H. Chao, J.-F. Jheng, J.-S. Wu, K.-Y. Wu, H.-H. Peng, M.-C. Tsai, C.-L. Wang, Y.-N. Hsiao, C.-L. Wang, C.-Y. Lin, C.-S. Hsu, *Adv. Mater.* **2014**, *26*, 5205.

[49] J. Zhou, X. Wan, Y. Liu, G. Long, F. Wang, Z. Li, Y. Zuo, C. Li, Y. Chen, *Chem. Mater.* **2011**, *23*, 4666.

[50] L. Fu, H. Pan, T. T. Larsen-Olsen, T. R. Andersen, E. Bundgaard, F. C. Krebs, H.-Z. Chen, *Dyes Pigm.* **2013**, *97*, 141.

[51] K.-H. Kim, H. Yu, H. Kang, D. J. Kang, C.-H. Cho, H.-H. Cho, J. H. Oh, B. J. Kim, *J. Mater. Chem. A* **2013**, *1*, 14538.

[52] D. Ye, X. Li, L. Yan, W. Zhang, Z. Hu, Y. Liang, J. Fang, W.-Y. Wong, X. Wang, *J. Mater. Chem. A* **2013**, *1*, 7622.

[53] J. Min, Y. N. Luponosov, N. Gasparini, L. Xue, F. V. Drozdov, S. M. Peregudova, P. V. Dmitryakov, K. L. Gerasimov, D. V. Anokhin, Z.-G. Zhang, T. Ameri, S. N. Chvalun, D. A. Ivanov, Y. Li, S. A. Ponomarenko, C. J. Brabec, *J. Mater. Chem. A* **2015**, *3*, 22695.

[54] C. D. Wessendorf, G. L. Schulz, A. Mishra, P. Kar, I. Ata, M. Weidelener, M. Urdanpilleta, J. Hanisch, E. Mena-Osteritz, M. Lindén, E. Ahlswede, P. Bäuerle, *Adv. Energy Mater.* **2014**, *4*, 1400266.

[55] M. Li, W. Ni, H. Feng, B. Kan, X. Wan, Y. Zhang, X. Yang, Y. Chen, *Chin. J. Chem.* **2015**, *33*, 852.

[56] Y. N. Luponosov, J. Min, A. V. Bakirov, P. V. Dmitryakov, S. N. Chvalun, S. M. Peregudova, T. Ameri, C. J. Brabec, S. A. Ponomarenko, *Dyes Pigm.* **2015**, *122*, 213.

[57] W. Ni, M. Li, F. Liu, X. Wan, H. Feng, B. Kan, Q. Zhang, H. Zhang, Y. Chen, *Chem. Mater.* **2015**, *27*, 6077.

[58] J. Min, X. Jiao, I. Ata, A. Osvet, T. Ameri, P. Bäuerle, H. Ade, C. J. Brabec, *Adv. Energy Mater.* **2016**, *6*, 1502579.

[59] R. Dominguez, N. F. Montcada, P. de la Cruz, E. Palomares, F. Langa, *Phys. Chem. Chem. Phys.* **2017**, *19*, 3640.

[60] V. Gupta, A. K. K. Kyaw, D. H. Wang, S. Chand, G. C. Bazan, A. J. Heeger, *Sci. Rep.* **2013**, *3*, 1965.

[61] H. Bai, Y. Wang, P. Cheng, Y. Li, D. Zhu, X. Zhan, *ACS Appl. Mater. Interfaces* **2014**, *6*, 8426.

[62] Q. Tan, X. Yang, M. Cheng, H. Wang, X. Wang, L. Sun, *J. Phys. Chem. C* **2014**, *118*, 16851.

[63] M. Cheng, X. Yang, C. Chen, Q. Tan, L. Sun, *J. Mater. Chem. A* **2014**, *2*, 10465.

[64] W. Ni, M. Li, B. Kan, Y. Zuo, Q. Zhang, G. Long, H. Feng, X. Wan, Y. Chen, *Org. Electron.* **2014**, *15*, 2285.

[65] H. Feng, M. Li, W. Ni, F. Liu, X. Wan, B. Kan, Y. Wang, Y. Zhang, Q. Zhang, Y. Zuo, X. Yang, Y. Chen, *J. Mater. Chem. A* **2015**, *3*, 16679.

[66] M. Li, W. Ni, H. Feng, X. Wan, Y. Liu, Y. Zuo, B. Kan, Q. Zhang, Y. Chen, *Org. Electron.* **2015**, *24*, 89.

[67] W. Wang, P. Shen, X. Dong, C. Weng, G. Wang, H. Bin, J. Zhang, Z. G. Zhang, Y. Li, *ACS Appl. Mater. Interfaces* **2017**, *9*, 4614.

[68] S. Kirchmeyer, K. Reuter, *J. Mater. Chem.* **2005**, *15*, 2077.

[69] N. F. Montcada, B. Pelado, A. Viterisi, J. Albero, J. Coro, P. d. l. Cruz, F. Langa, E. Palomares, *Org. Electron.* **2013**, *14*, 2826.

[70] N. F. Montcada, R. Dominguez, B. Pelado, P. d. l. Cruz, E. Palomares, F. Langa, *J. Mater. Chem. A* **2015**, *3*, 11340.

[71] S. M. Tuladhar, M. Azzouzi, F. Delval, J. Yao, A. A. Y. Guilbert, T. Kirchartz, N. F. Montcada, R. Dominguez, F. Langa, E. Palomares, J. Nelson, *ACS Energy Lett.* **2016**, *1*, 302.

[72] B. Y. Antwi, R. G. D. Taylor, J. Cameron, R. B. Owoare, R. Kingsford-Adaboh, P. J. Skabara, *RSC Adv.* **2016**, *6*, 98797.

[73] X.-W. Zhu, K. Lu, H. Li, R.-M. Zhou, Z.-X. Wei, *Chin. Chem. Lett.* **2016**, *27*, 1271.

[74] X. Zhu, B. Xia, K. Lu, H. Li, R. Zhou, J. Zhang, Y. Zhang, Z. Shuai, Z. Wei, *Chem. Mater.* **2016**, *28*, 943.

[75] M. Li, K. Gao, X. Wan, Q. Zhang, B. Kan, R. Xia, F. Liu, X. Yang, H. Feng, W. Ni, Y. Wang, J. Peng, H. Zhang, Z. Liang, H.-L. Yip, X. Peng, Y. Cao, Y. Chen, *Nat. Photonics* **2017**, *11*, 85.

[76] a) K. Cnops, B. P. Rand, D. Cheyns, B. Verreet, M. A. Empl, P. Heremans, *Nat. Commun.* **2014**, *5*, 3406; b) Y. Lin, J. Wang, Z. G. Zhang, H. Bai, Y. Li, D. Zhu, X. Zhan, *Adv. Mater.* **2015**, *27*, 1170; c) D. Sun, D. Meng, Y. Cai, B. Fan, Y. Li, W. Jiang, L. Huo, Y. Sun, Z. Wang, *J. Am. Chem. Soc.* **2015**, *137*, 11156; d) H. Bin, L. Gao, Z. G. Zhang, Y. Yang, Y. Zhang, C. Zhang, S. Chen, L. Xue, C. Yang, M. Xiao, Y. Li, *Nat. Commun.* **2016**, *7*, 13651; e) L. Gao, Z. G. Zhang, L. Xue, J. Min, J. Zhang, Z. Wei, Y. Li, *Adv. Mater.* **2016**, *28*, 1884.

[77] F. Zhao, S. Dai, Y. Wu, Q. Zhang, J. Wang, L. Jiang, Q. Ling, Z. Wei, W. Ma, W. You, C. Wang, X. Zhan, *Adv. Mater.* **2017**, *29*, 1700144.

[78] O. K. Kwon, J. H. Park, D. W. Kim, S. K. Park, S. Y. Park, *Adv. Mater.* **2015**, *27*, 1951.

[79] S. Badgujar, C. E. Song, S. Oh, W. S. Shin, S.-J. Moon, J.-C. Lee, I. H. Jung, S. K. Lee, *J. Mater. Chem. A* **2016**, *4*, 16335.

[80] L. Yang, S. Zhang, C. He, J. Zhang, H. Yao, Y. Yang, Y. Zhang, W. Zhao, J. Hou, *J. Am. Chem. Soc.* **2017**, *139*, 1958.

[81] H. Bin, Y. Yang, Z.-G. Zhang, L. Ye, M. Ghasemi, S. Chen, Y. Zhang, C. Zhang, C. Sun, L. Xue, C. Yang, H. Ade, Y. Li, *J. Am. Chem. Soc.* **2017**, *139*, 5085.

[82] M. C. Scharber, D. Mühlbacher, M. Koppe, P. Denk, C. Waldauf, A. J. Heeger, C. J. Brabec, *Adv. Mater.* **2006**, *18*, 789.

[83] S. R. Cowan, A. Roy, A. J. Heeger, *Phys. Rev. B* **2010**, *82*, 245207.

[84] T. M. Burke, S. Sweetnam, K. Vandewal, M. D. McGehee, *Adv. Energy Mater.* **2015**, *5*, 1500123.

[85] A. Zampetti, A. H. Fallahpour, M. Dianetti, L. Salamandra, F. Santoni, A. Gagliardi, M. Auf der Maur, F. Brunetti, A. Reale, T. M. Brown, A. Di Carlo, *J. Polym. Sci., Part B: Polym. Phys.* **2015**, *53*, 690.

[86] B. C. Thompson, J. M. J. Fréchet, *Angew. Chem., Int. Ed.* **2008**, *47*, 58.

[87] F. Liu, Y. Gu, X. Shen, S. Ferdous, H.-W. Wang, T. P. Russell, *Prog. Polym. Sci.* **2013**, *38*, 1990.